THE GEOLOGY OF THE OCEANOGRAPHER TRANSFORM: THE RIDGE-TRANSFORM INTERSECTION

OTTER

(Oceanographer Tectonic Research Team)

J. A. KARSON[1], P. J. FOX[2], H. SLOAN[2], K. T. CRANE[3], W. S. F. KIDD[4], E. BONATTI[3], J. B. STROUP[4], D. J. FORNARI[3], D. ELTHON[5], P. HAMLYN[3], J. F. CASEY[5], D. G. GALLO[2], D. NEEDHAM[6], and R. SARTORI[3]

(Accepted 28 August, 1983)

Abstract. Seven dives in the submersible ALVIN and four deep-towed (ANGUS) camera lowerings have been made at the eastern ridge-transform intersection of the Oceanographer Transform with the axis of the Mid-Atlantic Ridge. These data constrain our understanding of the processes that create and shape the distinctive morphology that is characteristic of slowly-slipping ridge-transform-ridge plate boundaries. Although the geological relationships observed in the rift valley floor in the study area are similar to those reported for the FAMOUS area, we observe a distinct change in the character of the rift valley floor with increasing proximity to the transform. Over a distance of approximately ten kilometers the volcanic constructional terrain becomes increasingly more disrupted by faulting and degraded by mass wasting. Moreover, proximal to the transform boundary, faults with orientations oblique to the trend of the rift valley are recognized. The morphology of the eastern rift valley wall is characterized by inward-facing scarps that are ridge-axis parallel, but the western rift valley wall, adjacent to the active transform zone, is characterized by a complex fault pattern defined by faults exhibiting a wide range of orientations. However, even for transform parallel faults no evidence for strike-slip displacement is observed throughout the study area and evidence for normal (dip-slip) displacement is ubiquitous. Basalts, semi-consolidated sediments (chalks, debris slide deposits) and serpentinized ultramafic rocks are recovered from localities within or proximal to the rift valley. The axis of accretion – principal transform displacement zone intersection is not clearly established, but appears to be located along the E–W trending, southern flank of the deep nodal basin that defines the intersection of the transform valley with the rift floor.

1. Introduction

The accretionary axis of the world-encircling mid-oceanic ridge system has been the focus of several detailed investigations (Mid-Atlantic Ridge at the FAMOUS area; Mid-Cayman Rise; Galapagos Rift; East Pacific Rise at 21° N) and the results of those studies have contributed greatly to our understanding of the processes that shape accretionary plate boundaries. A key tectonic feature of accreting plate boundaries is their offset at intervals by transform faults which are characterized by some of the roughest topography in the ocean basins. Wilson (1965) defined transform faults as plate boundaries along which there is translation, but where lithosphere is neither created nor destroyed. Investigations of

[1] Woods Hole Oceanographic Institution, Woods Hole, MA 02543, U.S.A.
[2] Graduate School of Oceanography, University of Rhode Island, Narragansett, RI 02882, U.S.A.
[3] Lamont-Doherty Geological Observatory, Palisades, NY 10964, U.S.A.
[4] Dept. of Geol. Sciences, SUNY at Albany, Albany, NY 12222, U.S.A.
[5] Dept. of Geology, University of Houston, TX 77004, U.S.A.
[6] C.O.B., B.P. 337, Brest, France.

Marine Geophysical Researches **6** (1984) 109–141. 0025-3235/84/0062-0109 $04.95

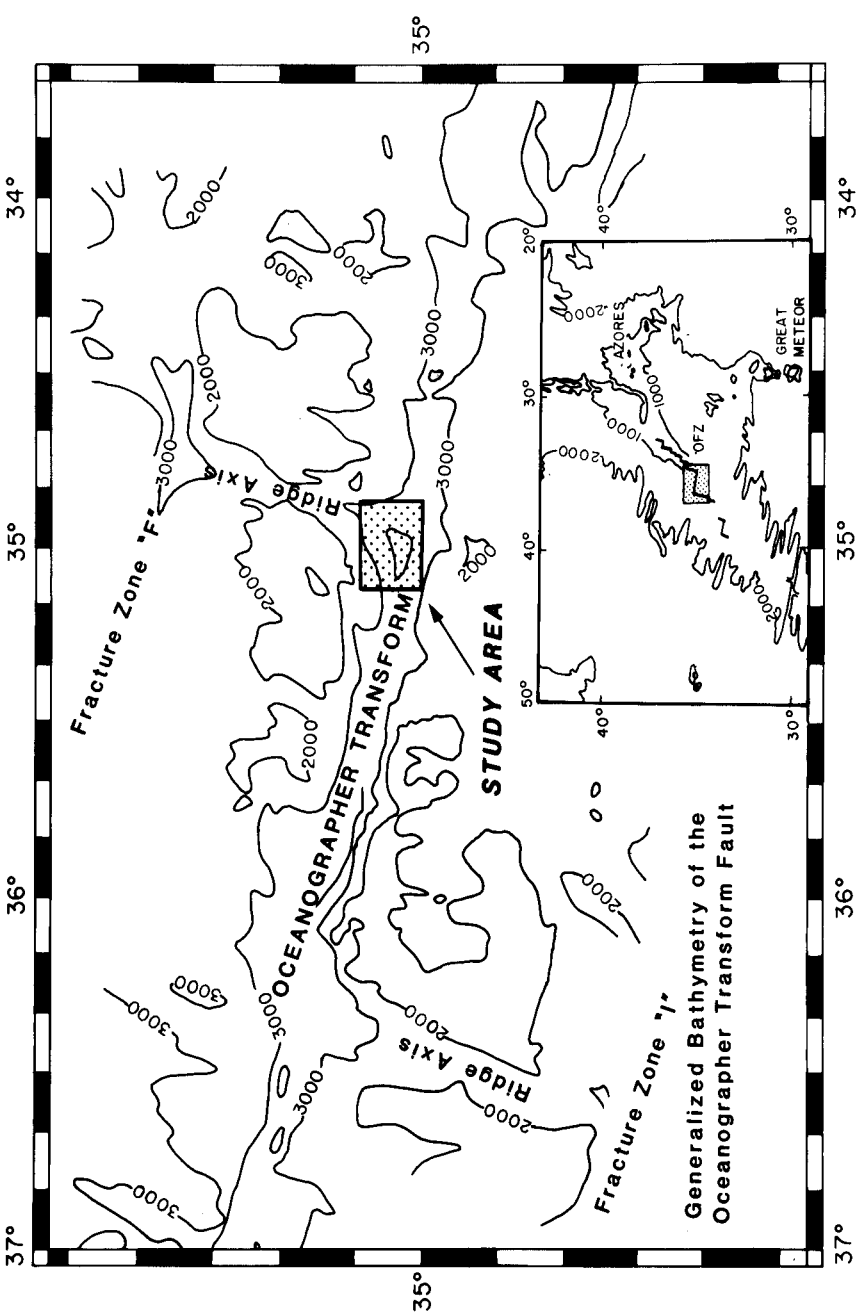

Fig. 1. Index map showing location of the Oceanographer Transform and a generalized bathymetric map of the Oceanographer Transform indicating the location of the investigation discussed in this paper. Depth in m.

transform faults indicate that Wilson's definition serves as a valid kinematic model but that in detail these plate boundaries are geologically complex (e.g. Menard and Atwater, 1968; Fox *et al.*, 1976; Francheteau *et al.*, 1976; Karson and Dewey, 1978).

In the summer of 1980 an investigation of the Oceanographer Fracture Zone (OFZ; 35° N, 35° W) and its eastern intersection with the Mid-Atlantic Ridge was conducted using the ANGUS deep-towed camera package and the manned submersible DSRV ALVIN (Figure 1). The purpose of this field program was to use the high-resolution capabilities of the submersible and deep-towed camera to address a family of questions fundamental to our understanding of the ridge-transform-ridge domain. The study was designed to: (1) define the styles of deformation that are characteristic of a large-offset, slowly-slipping transform fault; (2) investigate the structures developed at and proximal to the ridge axis-transform fault boundary; (3) establish the vertical and lateral distribution of rock types exposed along the transform valley walls and on the rift valley walls near the transform intersection.

Our field program was conducted in two areas in the Oceanographer Transform. One field area is located approximately midway between the offset segments of the Mid-Atlantic Ridge and the other is located at the eastern Oceanographer-Mid-Atlantic Ridge intersection. Our discussion in this paper concentrates on our results from the study of the ridge-transform intersection (Figure 1) and another companion paper will present the results obtained from the area at the center of the transform (OTTER, in prep.).

1.1. Field methods

Before presenting our geological observations we briefly review the strengths and limitations of the tools used to collect our field data. Photographic swaths of the sea floor were made using the ANGUS deep-towed camera system that exposes up to 400 feet of 35 mm film during a single lowering. The instrument is towed at speeds of 0.75 to 1.5 kts and in our survey was set to photograph at 20 sec intervals, so that a maximum of 30 km of sea floor were traversed during a lowering. The camera height above the bottom is monitored acoustically and is controlled by paying out or retrieving wire with the ship's winch. The camera is oriented vertically and when flying at an optimum height of 10 m the area photographed is approximately 13×18 m. In rough terrain, however, the height of the camera varies considerably from frame to frame because it is difficult to keep the camera height stable and valuable data is often lost in very steep terrain.

Many of our ANGUS traverses or parts of traverses were navigated acoustically within a bottom-moored transponder net located near the ridge-transform intersection. Within the net the camera sled's position with respect to the net is determined to within a few meters. The position of the net relative to the latitude and longitude of the base map is determined by fitting the transponder positions to the numerous satellite fixes obtained during the survey. When outside the range of

the transponder array, the towing ship's position was determined by radar ranges and bearings to the second ship (LULU) positioned in the net. Combined towing-ship and camera-sled navigation within the net shows that, except during turns, the sled accurately tracks the ship's path with a fixed offset directly behind the ship. Thus, the camera sled's position is fairly well determined (probably ±100 m) even when outside the range of acoustic navigation. This enabled our survey to cover a much larger area than that permitted by the net alone. Ship's time is recorded on each photograph and on the navigation record so that individual photographs can be positioned along the path of the ANGUS sled. The asimuth of the sled at a given time has been assumed to be parallel to the ship's path at that time. Preliminary measurements made with a magnetic compass on the sled tend to support this view and we believe that the orientation of features in our photographs can be estimated to within ±10°, which is sufficient for our analysis.

Data recorded from the manned-submersible ALVIN include direct observations, continuous black and white video-taped views of the sea floor, as well as color photographs from external hull-mounted cameras and some hand-held cameras inside. Side-scanning sonar was also used from ALVIN to define the lateral extent and azimuth of scarps encountered on the sea floor. The submarine's position was determined by acoustic navigation within the transponder net. Heading was accurately determined by a gyro-compass and is recorded on external camera photos that are keyed to time in order to orient and position geological features on the sea floor. Rock and sediment samples were collected from outcrops and nearby talus piles by the use of ALVIN's mechanical arm.

One of the goals of this study was to map the distribution and geometry of fault zones near the ridge-transform intersection. The identification and interpretation of faults from surface observations, however, is not always a simple matter. Our observations typically show that the volcanic constructional terrain or sediment-covered areas are interrupted by steep outcrops with slopes ranging from subvertical to 30°. Individual scarps range from a few centimeters to a few tens of meters in height. Slopes of less that 30° are nearly always covered with a smooth veneer of calcareous pelagic ooze that is often dotted with talus. In areas where talus is especially abundant, the origin and magnitude of these scarps may be ambiguous. We therefore choose to use non-genetic terms in describing them. In general, we believe that most of these scarps are the surface expression, albeit often degraded and modified by mass wasting, of steeply dipping faults with some dip-slip displacement. This interpretation is supported by several observations. The lateral continuity (tens of meters to >1.0 km) and linear aspect of the scarps strongly supports a tectonic origin. Direct observations of scarps from ALVIN often provide additional geologic constraints that indicate faulting, including the exposure of fresh, unweathered rock even in relatively old terrain, sediment-free talus ramps at the foot of the scarp, coarse grooves and striae suggestive of slickensides, and truncated geologic structures (e.g. bedding, lava flows, older faults, etc.).

2. Morphology of the Eastern Ridge-Transform Intersection from Surface Observations

The first-order morphology of the Oceanographer Fracture Zone – Mid-Atlantic Ridge (MAR) intersection, as defined by conventional, surface-ship bathymetry, is described in detail elsewhere (Fox *et al.*, 1969; Schroeder, 1977; Williams *et al.*, 1983; Fox *et al.*, in review) but is briefly summarized here in order to put our detailed data in a regional perspective. South of the Azores triple junction the MAR is characterized by short (60 to 100 km) ridge segments that are offset by a few tens of kilometers to many tens of kilometers by transform faults (Phillips and Fleming, 1978). At 35° N the Oceanographer Transform is a well-defined, east-west trending bathymetric feature offsetting the ridge axis by 130 km. The sense of ridge offset is dextral and, therefore, the sense of strike-slip displacement across the transform should be sinistral. The floor of the steep-walled transform valley is composed of a number of elongate, closed-contour depressions. The shallowest point of the transform valley floor (~3400 m) is located near the mid-point between the ridge-transform intersections which are characterized by deep (>4500 m), closed-contour depressions or nodal basins. The regional trend of the transform valley is approximately ESE–WNW but this morphotectonic grain is a composite of several 20–30 km long troughs that exhibit trends ranging from 075° to 110° (Fox *et al.*, in review).

The rift valley of the MAR to the north of the Oceanographer Transform trends 015° and is characterized by a *V*-shaped valley that is 85 km long and is truncated at its northern end by a small (30 km offset) left-lateral transform called Fracture Zone F (Fox *et al.*, 1969; Phillips *et al.*, 1975). At a point approximately midway between these two transforms the rift valley floor is shallow (2206 m) and narrow but the floor of the rift deepens and widens continuously over distances of 40 km towards the transforms (Schroeder, 1977; Fox *et al.*, in review). Closed-contour depth maximums are recognized at the rift valley-transform intersections with a depth of 4670 m recorded at the Oceanographer intersection. The median valley wall adjacent to the Oceanographer Transform is up to 500 m higher than the opposing median valley wall which is adjacent to the aseismic eastern limb of the fracture zone.

A multi-narrow beam echo-sounding (Sea Beam) survey of a portion of the eastern intersection of the OFZ was made by the JEAN CHARCOT (Needham, unpublished data) and these data were combined with existing, conventional wide beam echo-sounding information to produce a detailed bathymetric map of the study area (Figure 2). The survey concentrated on the broad, triangular shaped basin that dominates the intersection morphology. At the very northern limit of the survey area (35° 10′ N) the floor of the rift valley is narrow (2 km) and bounded to the east and west by inward facing, NNE–SSW (015°) linear steps that define the rift valley walls. From this point southwards over the next 16 km the morphology of the rift valley changes continuously and systematically as the transform boundary is

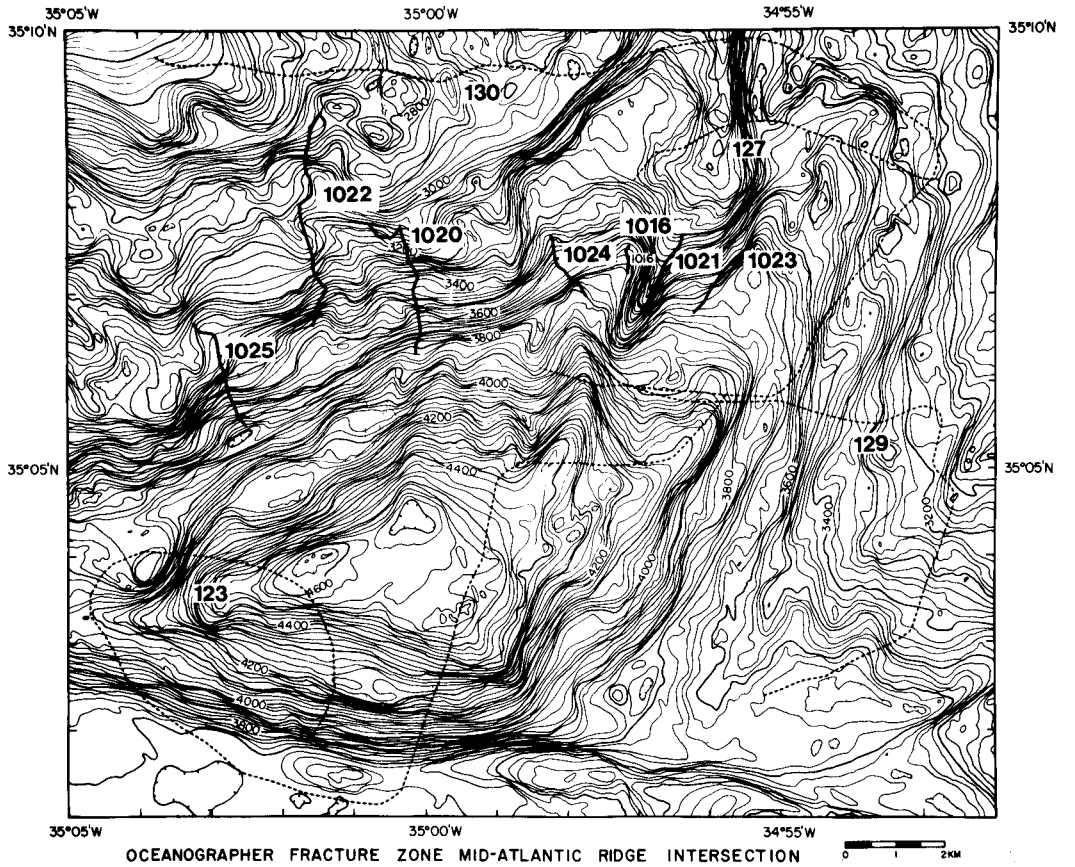

Fig. 2. Bathymetric map of the eastern intersection of the Oceanographer Transform with the Mid-Atlantic Ridge. Map is constrained by Sea Beam data collected by the JEAN CHARCOT (Needham, unpublished data) and by conventional echo sounding profiles. Depth in m; dotted lines indicate deep-towed photographic traverses (ANGUS – lowerings 123, 127, 129, 130); solid lines indicate submersible traverses (ALVIN – Dives 1016, 1020–1025).

approached. With increasing proximity to the transform the depth to the rift valley floor increases rapidly, and the morphology of the rift evolves into a broad, asymmetric U-shaped valley. To the east of the valley axis the rift walls retain the NNE–SSW morphologic grain of the ridge axis. In these areas the sea floor rises in a step-like fashion above the median valley floor with broad 1–2 km wide, inward-sloping terraces linking narrow, 1 km wide intervals of steep relief. At its southern terminus the east wall of the rift valley is abruptly truncated by and forms a right-angle corner with the north side of the ESE–WNW (100°) striking eastern limb of the OFZ.

In marked contrast to the eastern rift-valley wall, the western wall is composed of terrain elements that create a well-defined NE–SW fabric that is oblique to both the regional strike of the ridge axis and the Oceanographer Transform (Schroeder,

1977; Figure 2). Numerous, steep southeast-facing blocks with relief of a few hundred meters and with continuity along strike of several kilometers highlight the morphology, but this topographic expression is interrupted in places by short, steep lineaments that strike E–W or N–S and by broad, sloping platforms with complex undulating relief. At the northern limits of our survey the strike of the west wall is approximately 045°, but with increasing proximity to the transform intersection, 070° trends become dominant. Interestingly, the lineated topographic grain of the rift wall is best defined between the 4000 to 3000 m depth interval. Above 3000 m a distinct regional grain is muted by the occurrence of equidimensional peaks and depressions. These non-linear features are also recognized on the eastern side of the valley, but do not occur as frequently.

The morphology of the rift valley floor is dominated by the regional, southwest plunge of the sea-floor towards the nodal basin; from the northern limit of our survey area to the southern side of the nodal basin, over a distance of 16 km, the depth increases by 1400 m. Superimposed upon this regional slope are irregularly shaped elongate ridges, troughs, lines of domes, and depressions that are aligned approximately parallel to the regional trend of the MAR axis (015°). The most prominent feature of the valley floor is an eight kilometer-long ridge that, at the northern end of the survey area, is rather broad with only a few hundred meters of relief but that, to the south, becomes increasingly better defined as a narrow 400 m-high knife-edge ridge, until it pinches out on the western flank of a steep-sided trough.

A closed-contour intersection deep, or nodal basin, is clearly defined by the 4100 m contour and has a distinctive triangular shape: the strike of the eastern side is roughly parallel to the trend of the ridge axis, the western flank of the basin mimics the oblique NE–SW trends of the western rift wall, and the southern side parallels the regional trend of the Oceanographer Transform and defines the base of the south wall of the transform valley. The center of the basin appears to be positioned a few kilometers to the west of the point at which the MAR axis, if projected due south, would intersect the transform valley axis. The sides of the nodal basin are steep and create 400 to 500 m of relief; below 4500 m the basin floor is smoothed by ponded sediments up to 100 m in thickness (Schroeder, 1977).

3. Ridge-Transform Intersection: Near-Bottom Observations

Kinematics of accreting plate boundaries predict that ridge-transform intersections should be composed of 5 distinct morphotectonic zones that are characterized by contrasting styles of tectonism: the axis of accretion defined by the floor of the rift valley; the non-transform side of the rift valley; the transform flank of the rift valley; the transform valley, containing the zone of active transform tectonism (principal transform displacement zone or PTDZ); and the aseismic extension or non-transform section of the fracture zone. Our field program was designed to

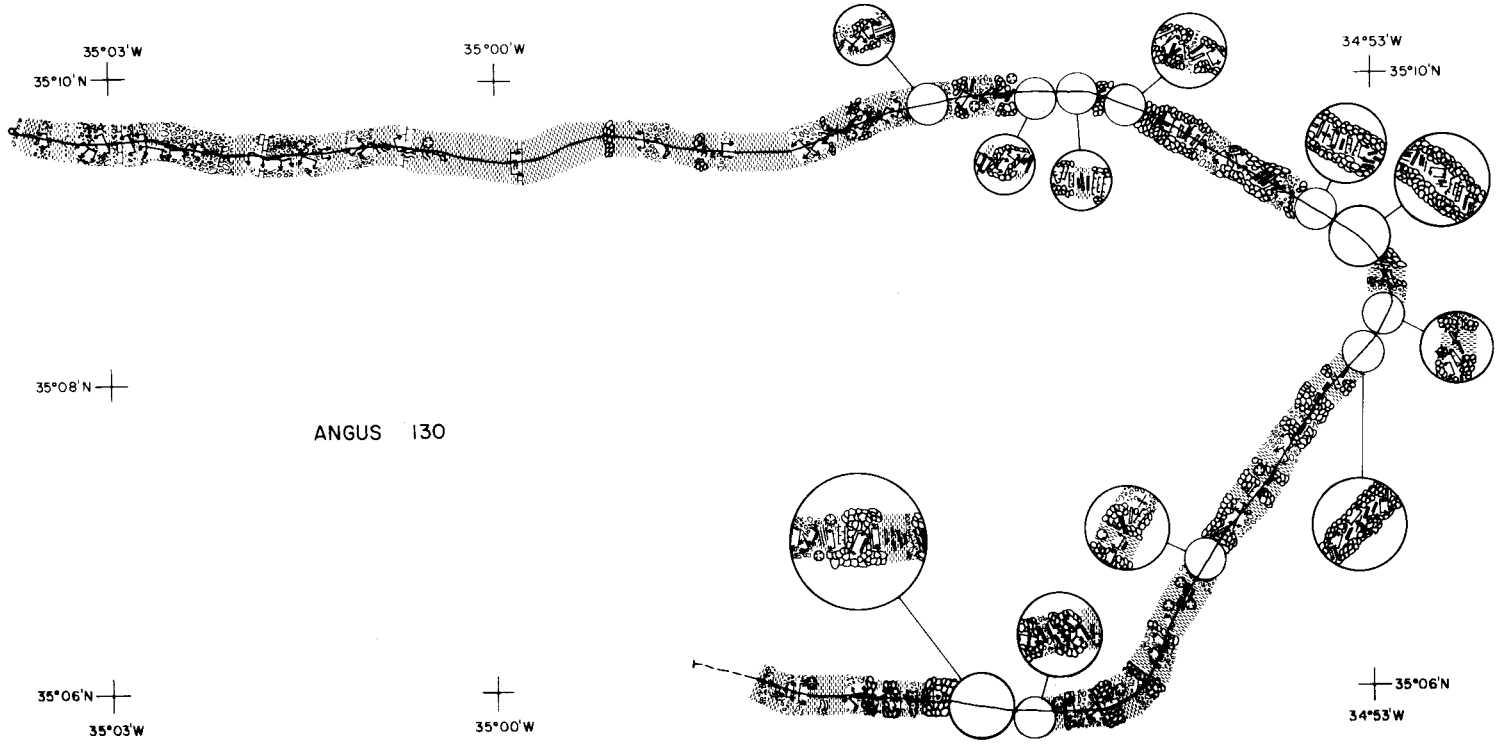

Fig. 3. ANGUS traverse 130 across the floor of the rift valley; see Figure 2 for location and Figure 4 for the key to the symbols used.

explore the surface geology of the first four of these tectonic zones. In this section we summarize our observations concerning sedimentary processes, the nature of the volcanic constructional terrain, the distribution and geometry of tectonic features and the distribution of various sedimentary and igneous lithologies recovered.

3.1. The axis of accretion: the rift valley floor

Our interpretation of the processes that are shaping the rift-valley floor proximal to the Ocenaographer Transform fault is based on analysis of several ANGUS camera traverses (123, 127, 129, and 130; Figures 3, 4, 5, 6) and three ALVIN dives (1016, 1021, and 1023; Figure 7). The constructional volcanic features of the median-valley floor are similar to those in the volcanic terrain observed elsewhere at localities along the mid-oceanic ridge system (e.g. Ballard and van Andel, 1977, RISE, 1980; Ballard *et al.*, 1980; CYAMEX, 1981), but the volcanic features created in close proximity to the Oceanographer Transform boundary appear to be more disrupted by pervasive faulting (Figure 8).

The paucity of sediment cover and the glassy reflective nature of the extrusive material define the relatively narrow zone of recent volcanism that is situated along the eastern side of the median valley floor (Figure 9a). Broad exposures of bulbous pillows decorated with delicate lava ornaments and extrusion marks are the most abundant extrusive product and create an undulating seafloor surface. Ponded lavas were rarely observed but the existence of these lavas can be easily obscured by a thin veneer of sediment or talus.

Constructional mounds ('haystacks') and elongate ridges occur sporadically throughout the area. The mounds are conical in form with roughly circular bases up to a few tens of meters in diameter and with rounded peaks, and have relief ranging from 5 to 20 m. The outer layers of the mounds are constructed of tube-shaped lavas and elongate pillows that are apparently extruded near the summit. In some cases eruption of magma on the flanks of mounds has created an outer layer of tangled and overlapping lava tubes. Chains of these volcanic mounds and ridges tend to have a rather strong preferred orientation of 010° to 030°, nearly parallel to the regional trend of the MAR axis.

Steep asymmetric lava fronts, representing edges of lava flows and/or fault scarps mantled by lavas, are observed in a few places and are characterized by bulbous or tube-shaped pillows that end abruptly creating a steep wall with relief of several meters. Whole detached pillows as well as pillow fragments lie along the base of the flow fronts. In some places unbroken lava partially covers talus suggesting that the debris is overrun by advancing lava shortly after or during debris accumulation (Figure 9b).

Soon after emplacement and creation of the hummocky volcanic constructional terrain this topography is degraded and obscured by fissuring, faulting and mass wasting. In the northern part of the field area fissures tend to be associated with regions of very recent volcanism, but towards the south, where a relatively thick

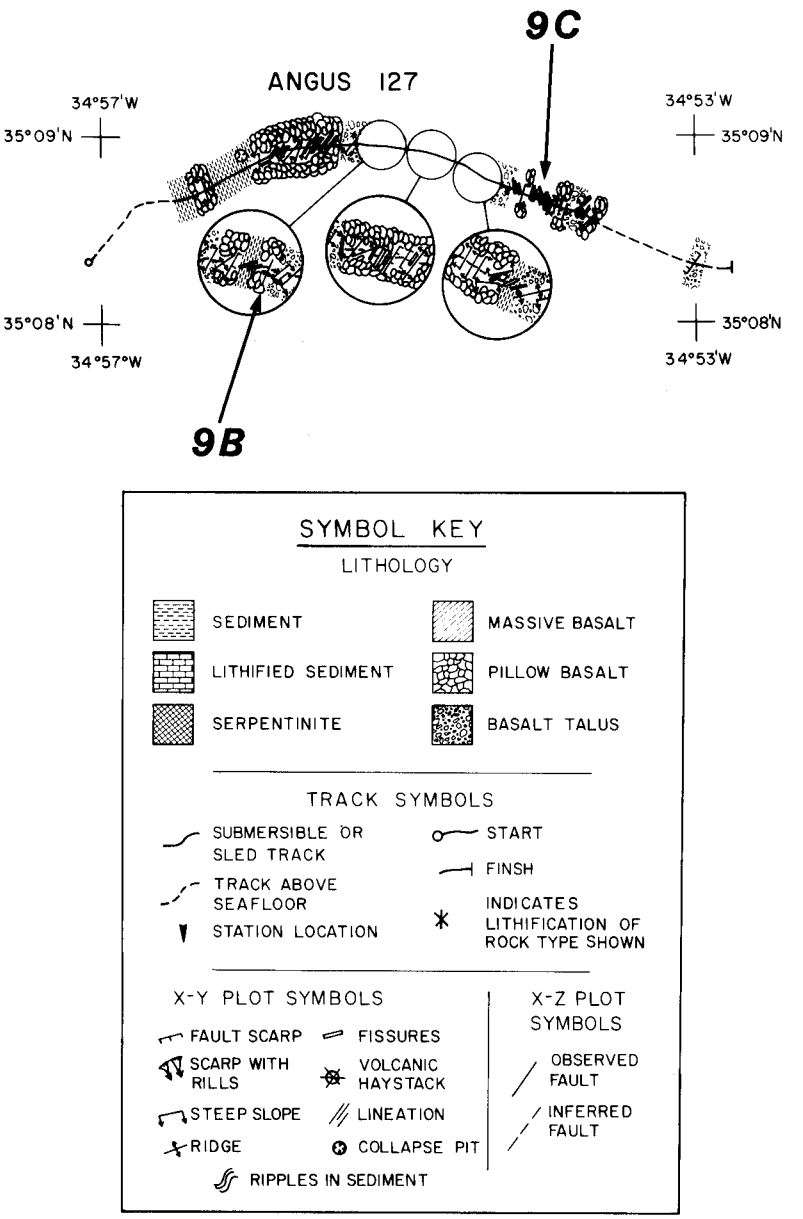

Fig. 4. ANGUS traverse 127 across rift floor and up eastern flank of rift valley wall; see Figure 2 for location.

blanket of sediment covers the basement flooring the nodal basin, fissures are observed to cut sediment (Figure 9c). The fissures range from 0.5 to 5.0 m in width and have been traced laterally for up to several tens of meters. Their surface traces are more or less linear over distances of about 10 m, but in detail their walls are very irregular reflecting separation along local surfaces of weakness. The orien-

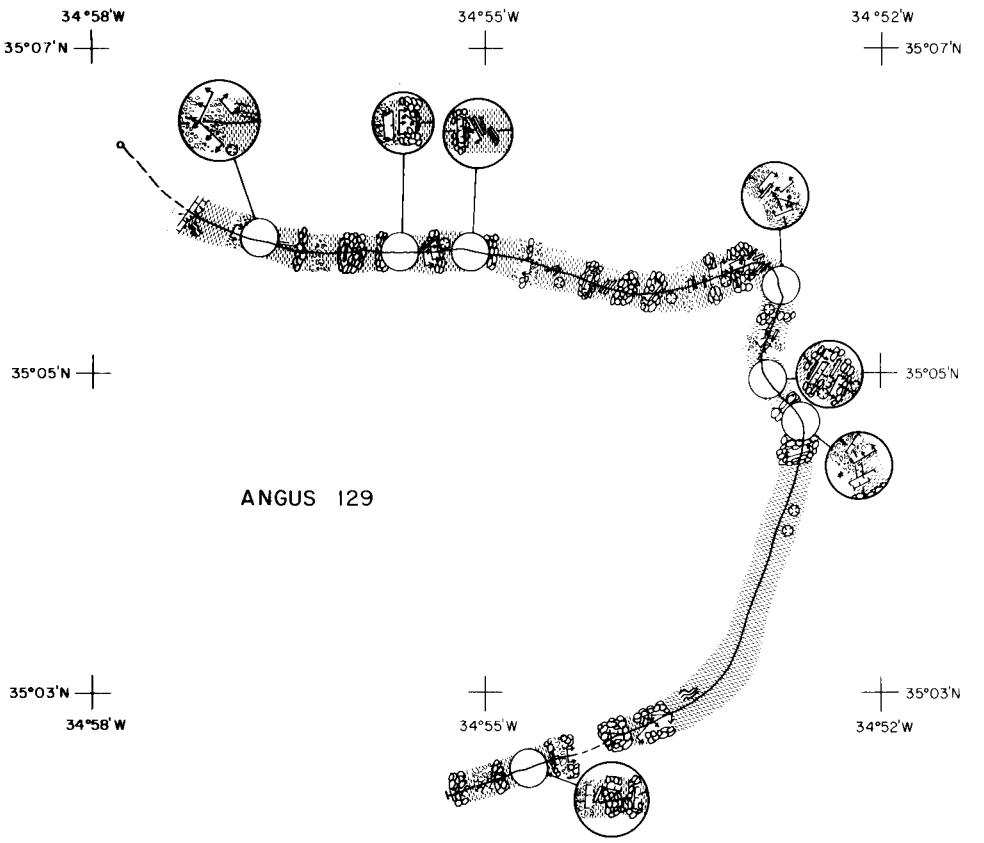

Fig. 5. ANGUS traverse 129 across rift floor and up eastern flank of rift valley wall; see Figure 4 for the key to symbols used.

tations of fissures range from 350° to 060° (Figure 8), but are dominantly subparallel to the ridge axis.

Fault scarps generally occur as steep rock walls from less than 1.0 m to a few tens of meters in height indicating that there has been significant dip-slip displacements across the faults (Figure 8). No evidence of oblique-slip or strike-slip motion was found, but this kind of motion is much harder to document. The scarps tend to have a linear trace on the seafloor and to be laterally continuous for tens of meters disappearing along strike into young volcanic terrain, beneath talus accumulations, at cross-cutting faults or by decrease of slip on the fault along strike. The scarps dissect sections of the median valley floor revealing truncated margins of lava pillows and tubes, talus, welded talus and breccias, basaltic dikes, massive sills and/or flows, and variably consolidated calcareous sediment. In a few places, older fault zones, marked by narrow, cross-cutting zones of breccia, were observed within the truncated intervals. From the synthesis of relationships observed on all our traverses, it appears that on a broad scale (hundreds of meters) these faults

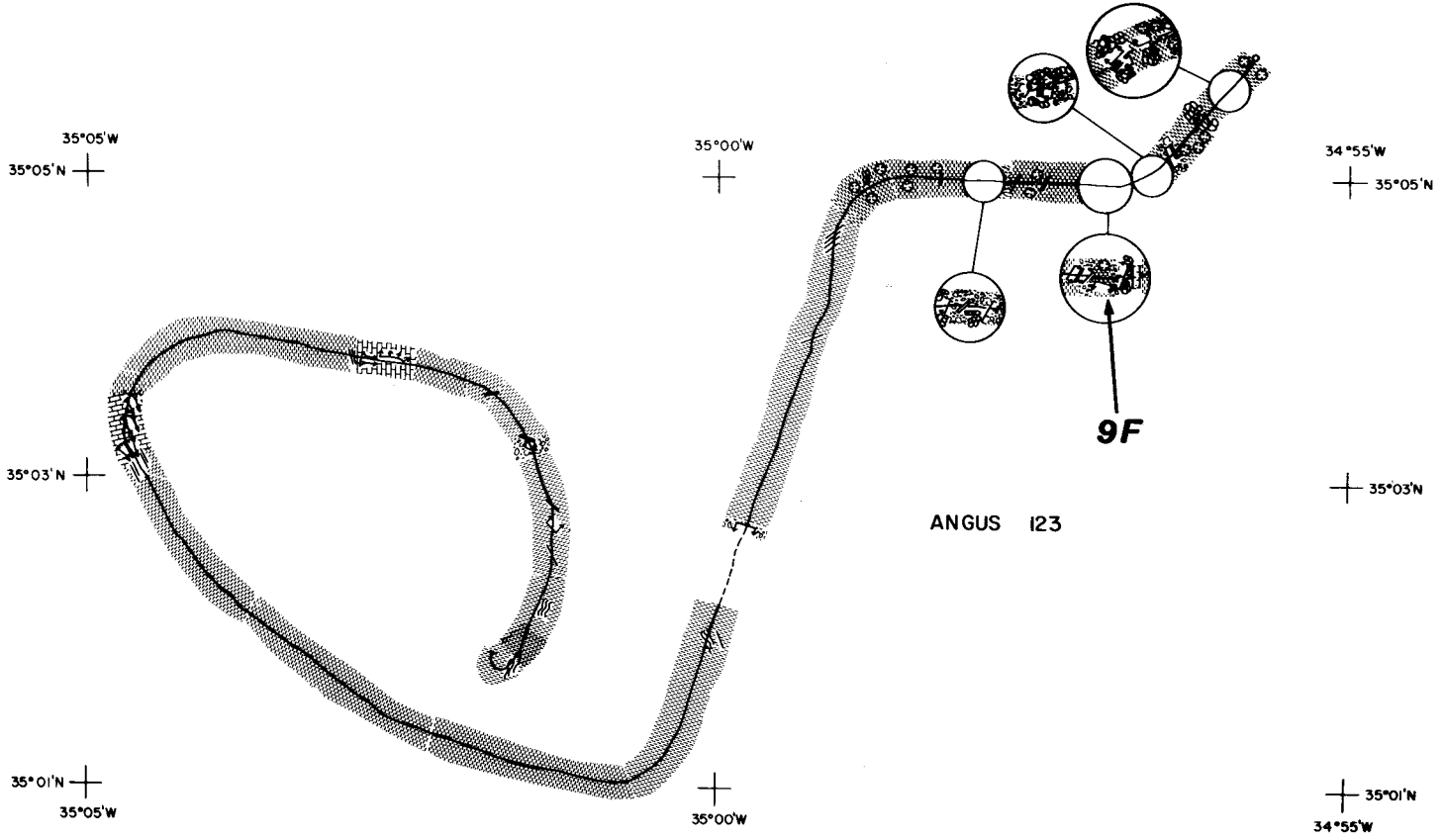

Fig. 6. ANGUS traverse 123 down rift floor, across nodal basin and along the axis of the Oceanographer Transform; see Figure 2 for location and Figure 4 for key to symbols used.

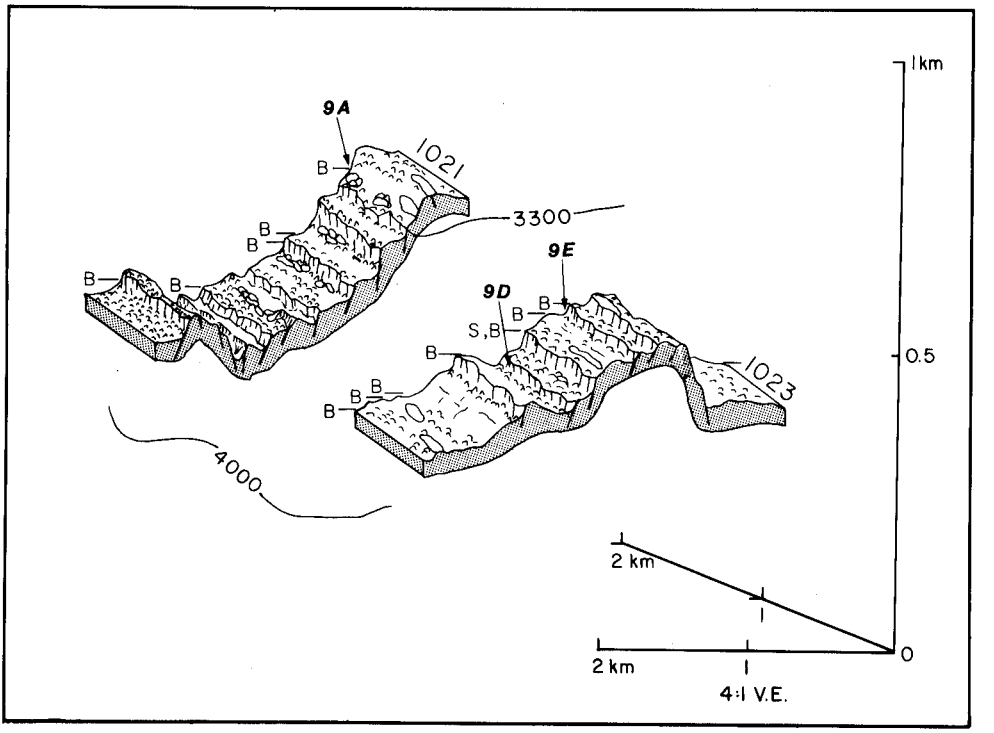

Fig. 7. Geologic reconstructions of ALVIN dives 1021 and 1023 along the rift valley floor (reference Figure 2 for locations; profile for dive 1016 not available due to insufficient navigation data). Sections are constructed by showing geology between two identical and offset dive profiles offset from each other perpendicular to the general track direction. This format permits the illustrations of features observed on either side of the submersible during the traverses. Letters S (sediment) and B (basalt) indicate sample locations; extrusive pavement (pillow lavas) and talus are indicated by discontinuous black lines; sediment patches shown as white areas; fault scarps are defined by steep lines but dip of faults is hypothetical. Depth in m.

integrate to produce the up-lifted and down-dropped blocks of horst and graben terrain that typifies the rift valley floor elsewhere on the MAR (Ballard and van Andel, 1977).

Faulting and fissuring appear to be quite widespread in the median valley floor (Figure 8) but our estimates of the density of these features represent a minimum. This is due to the action of several different processes that tend to obscure the nature and extent of faulting, including recent volcanism, talus accumulation, and the highly-fractured, loosely-packed character of the pillow-lava terrain. The porous, fragmental, rather incoherent volcanic pile apparently may respond to faulting near the surface by rotation and jostling of small-scale individual fragments rather than by the formation of a well-defined fault plane. Thus, although it cannot be unequivocally established from the available data, many steep slopes and ramps observed in the rubble and talus in this area may be the muted surface expression of faulting at depth within the more coherent basement.

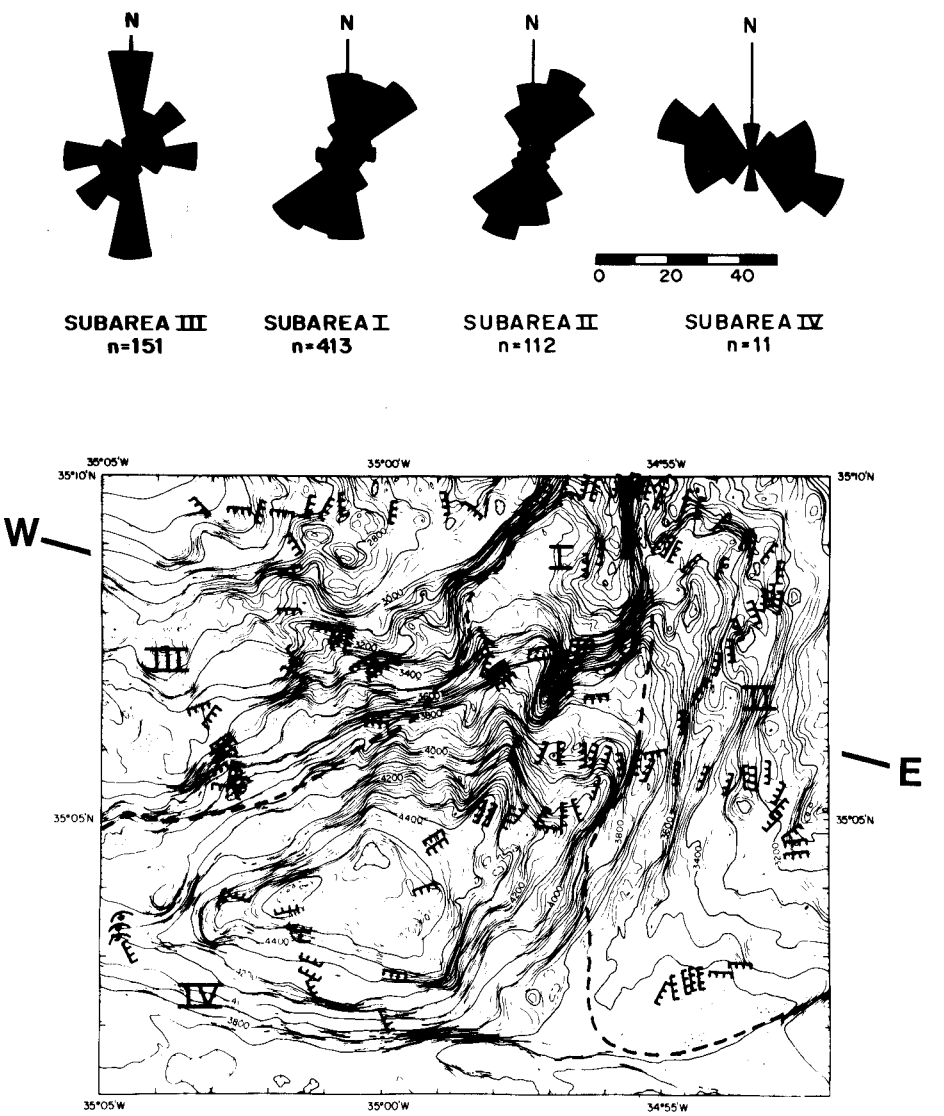

Fig. 8. Bathymetric map of the rift valley – transform intersection with generalized orientations of fault scarps observed along the ALVIN and ANGUS traverses (tick marks are down-thrown side of the faults). ROSE diagrams above map summarize the structural orientation data for each of the four tectonic provinces investigated (I – rift valley floor; II – eastern rift valley wall; III – western rift valley wall; IV – transform valley). Location of geologic cross-section shown in Figure 12 is indicated by letters E and W.

The overall structural grain of the median-valley floor appears to be variable both along strike from north to south and across strike from east to west, with respect to distance from the ridge-transform intersection. Along the axis of most recent volcanism the faults and fissures have orientations that are predominantly N–S, but it appears that the frequency of faults and diversity of fault orientation increase towards the transform intersection, as the N–S trending volcanic and structural grain of the rift floor is disrupted by E–W striking faults that step the sea floor down into the nodal basin. In the across-strike perspective, at the northern end of our survey area N–S striking faults and talus wedges are observed to flank the zone of recent volcanism. With increasing proximity to the rift-transform intersection the orientation of faults changes: to the east of the axis N–S trending, ridge-axis parallel faults are most often observed, but west of the axis approximately NE–SW trending faults are frequently encountered. There is no evidence to suggest that any of these fault traces, regardless of orientation, have accommodated anything but dip-slip motion.

The volcanic constructional and fault-bounded terrain of the rift-valley floor are rapidly modified and degraded by mass wasting. Basaltic talus consisting of accumulations of angular pillow lava fragments from a few centimeters to >1.0 m in diameter is a nearly ubiquitous feature of the seafloor in this area (Figure 9d). Indeed, broad expanses of talus covering hundreds of meters of traverse were observed throughout the region. In some places, very fresh, unweathered basalt blocks occur at the base of steep scarps (Figure 9e). The blocks include nearly whole lava pillows as well as wedge-shaped fragments with a radial joint pattern characteristic of talus derived from pillow lava. The ramps and aprons constructed by this material form at and build upward from the base of fault scarps, tending to smooth the local topography through the removal of material from the face of the scarps and the consequent burial of adjoining depressions. The presence of well-developed talus ramps along fault scarps in even the youngest, central part of the median valley demonstrates that the decay and collapse of scarps in the volcanic basement begins soon after these features are formed. As the volcanic carapace ages in the first few hundreds of thousands of years, wedge-shaped talus accumulations grow continuously, both laterally, as individual fans of rubble coalesce along the face of an escarpment, and vertically, as steeply-dipping (20°–40°) talus wedges climb upwards fed from eroding outcrops above.

Pelagic-sediment deposition is another process that mutes the basement relief of the valley floor. At the northern end of the survey area, unconsolidated, calcareous-rich pelagic ooze dusts the steep volcanic slopes, fills in the cracks between pillow lavas and blankets the hollows. As the intersection is approached, however, the amount of pelagic sediment and rubble increases markedly until, in the nodal basin below a depth of 4400 m, the sediment blanket is uninterrupted. No bedrock out-crops were observed in this region and seismic reflection profiler data indicates that the sediment could be on the order of 100 m thick (Schroeder, 1977; Fox *et al.*, under review). There are a few complimentary processes that lead to the

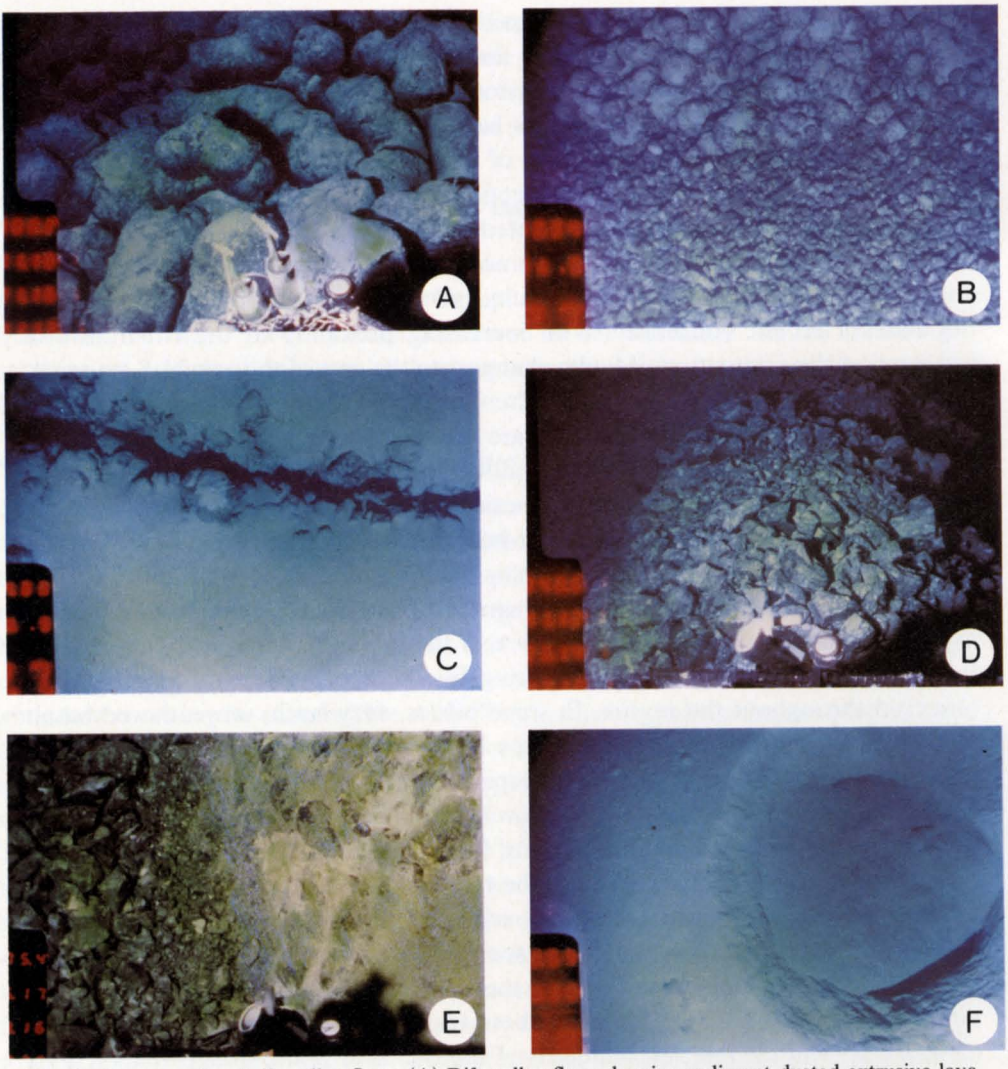

Fig. 9. Photographs of rift valley floor. (A) Rift valley floor showing sediment-dusted extrusive lava. Individual pillows are about 0.5 m across. (Hull-mounted camera, ALVIN dive 1021, time 16:41:13, depth 3290 m, see Figure 7 for location). (B) Rift valley floor showing fresh basalt talus in contact with a steep slope made up of extrusive lava. Field of view is about 10 m wide. (ANGUS photo, lowering 127; time 13:34:01; depth 3250 m; see Figure 4 for location). (C) Rift valley floor showing a fissure (about 1.0 m wide) that disrupts sediment covered extrusive terrain. Fissure strikes approximately N–S. (ANGUS photo, lowering 127; time 14:33:18; depth 3380 m; see Figure 4 for location). (D) Photograph of a narrow ridge on the rift floor made up of basaltic rubble that falls steeply off to the right and left; ridge axis strikes N–S and the view is towards the north. Field of view is about 4.0 m wide at the center. (Hull-mounted camera, ALVIN dive 1023; time 14:43:12; depth 3641 m; see Figure 7 for location). (E) E–W striking escarpment of relatively old, sedimented, pillow lava (consolidated talus?) in contact with fresh talus. Field of view is about 2.0 m across. (Hull-mounted camera, ALVIN dive 1023; time 16:28:26; depth 3556 m; see Figure 7 for location). (F) Large circular depression produced by the collapse of thick sediments into underlying void space in basement rocks; these are common features in the intersection nodal basin. The pit is about 3.0 m in diameter. (ANGUS photo, lowering 123; time 12:57:29; depth 4150 m; see Figure 6 for location).

development of an anomalously thick accumulation of sediment in the closed-contour nodal basin. First, the basin probably acts as a depositional focal point for pelagic sediment and mass-wasted debris shed from the high ground surrounding the basin. Furthermore, although there is little evidence to suggest current activity along the rift floor, we know from our investigations along the transform valley to the west that geostrophic bottom currents are an important process in redistributing pelagic sediment along the valley walls. The triangular-shaped intersection deep would interrupt the flow of currents moving along the fracture zone and act as a sink for pelagic sediment.

Circular depressions are frequently observed in sediment along the rift floor and range from about 0.5 to 10 m in diameter and from a few tens of centimeters to greater than 1.0 m in depth (Figure 9f). In general they appear to be about twice as wide as they are deep and are conical in form with sharp upper edges and steeply inclined walls. On these walls the subtle trace of subhorizontal light-brown to buff-colored bedding is visible and appears to be approximately 1–10 cm thick. The floors of the pits usually consist of a jumbled pile of semi-consolidated sediment fragments and smooth unconsolidated ooze. The collapse pits are often arranged in lines along or just behind the crest of steep scarps and slopes. We interpret these features to represent places where semi-consolidated calcareous sediment has collapsed into void space generated by faults and fissures in the under-lying volcanic basement. The position and alignment of collapse pits near some scarps suggests that these depressions may occur above fissures that are opening behind the scarps delineating the trace of zones of weakness along which material separates from the face of a steep fault scarp.

As the floor of the median valley ages, carbonate sediment and basaltic talus become mixed together as pelagic ooze sifts down into the talus wedges along open cracks and as down-slope processes mix pelagic sediment and basaltic debris. From observations of talus ramps and various breccias that are dissected by faults along the edges of the rift floor, it is apparent that chemical cementation and the welding of clasts is accomplished very soon after deposition and reflects the rapid precipitation of ferromanganese oxides and induration of interstitial carbonate. These processes will be greatly enhanced by the diffuse circulation of fluids at elevated temperatures through the talus piles. Cementation in talus piles is probably favored because talus is located along fault scarps that are likely to provide permeable pathways for hydrothermal outflow (Temple *et al.*, 1979; Rona, 1981).

Rock samples recovered along the rift valley floor include only basalts and variably consolidated calcareous sediments. The basalts range from aphyric to plagioclase and/or olivine phyric varieties. Brecciated and variably weathered basalts occur in the floor, but most are relatively fresh with glassy to partially palagonitized rims intact. A dredge haul from a previous cruise (V30–RD10; Fox *et al.*, 1976) in the rift valley floor at 3300 m depth recovered similar lithologies. A discussion of the geochemical characteristics and petrology of these basalts will be presented elsewhere (OTTER, in prep.).

3.2. The non-transform side of the rift: the eastern wall

Portions of ANGUS lowerings 127, 129 and 130 (Figures 3, 4, and 5) traversed the flanks of the eastern rift valley wall and established that this area is characterized by a series of NNE striking, west-facing intervals of relatively steep terrain that are linked by broad, 1km to 2km wide terraces (Figure 8); a morphology similar to that documented for other slowly accreting rift valley walls (e.g. Atwater, 1979; Stroup and Fox, 1981; Crane and Ballard, 1981). The steep intervals develop several tens to a few hundred meters of relief and define zones composed of a family of closely-spaced fault scarps that individually extend along strike for distances of a few tens to a few hundred meters each having relief of only a few meters to a few tens of meters. In isolation, individual rock escarpments appear to be badly degraded by mass wasting and to be relatively insignificant, but these fault scarps integrate spatially to create steps in the topography. The faults are generally west-facing although east-facing faults were observed in a few places. Fault scarps generally range from N–S to 040° with trends of 020° being most common. The diagnostic oblate shape of pillow lavas exposed in cross section on the faces of escarpments suggest that extrusive lavas are the dominant rock type.

Steeply sloping talus wedges composed of nearly whole lava pillows and angular rock fragments lap up against rock escarpments. Both relatively fresh, unconsolidated, sediment-free talus and partly sediment-covered talus were observed at the base of fault scarps. In some cases the talus breccias outcrop on subvertical slopes, demonstrating that induration of talus occurs even on very young crust and that the welded material is coherent enough to support a steep, fault-generated slope.

The terraces that link steep scarps are rather featureless areas characterized by a smooth, continuous blanket of pelagic carbonate that often contains scattered blocks of talus. The sediment-covered surfaces are devoid of evidence that suggests recent tectonic activity and have a gentle, overall slope towards the rift valley. On a small scale the terraces undulate in a complex manner suggesting that beneath the veneer of pelagic sediment lies a complex assemblage of debris that has been shed from steep terrain above. Although not well constrained by our data on this side of the valley, there may be a marked age progression in the evolution of rift valley terrain and the development of land forms. The base of the rift valley wall seems to be tectonically active with the development of near vertical scarps that expose fresh-looking extrusive rocks or welded talus. Farther upslope, scarps do not appear to be as steep or as numerous, talus aprons are dusted with sediment and sediment-covered terraces become well developed.

Overall, the morphology of the east wall of the rift valley is a product of two processes: the creation of step-like topography that strikes approximately parallel to the ridge axis along west-facing faults, and the pervasive and intensive mass wasting of volcanic constructional features and fault scarps. Any motion on the faults seems to take place largely at the base of the rift valley wall where packets of

crust are uplifted incrementally. In the absence of significant volcanism and faulting on the rift walls, mass wasting very quickly attenuates, rounds and smooths the morphotectonic fabric. A similar evolution for the rift valley walls of the Mid-Cayman Rise was proposed by Stroup and Fox (1981).

3.3. The transform side of the rift: the western wall

Our understanding of the geology of the western wall of the rift valley is constrained by 4 ALVIN dives (1020, 1022, 1024, 1025; Figure 10), part of ANGUS lowering 130 (Figure 3), and several dredge hauls. In the area where we positioned our dives the rift valley is distinctly U-shaped and the sea floor shallows continuously from the depths of the nodal basin to the crests of the flanking rift mountains. The western wall tectonic province is characterized by broad, undulating pelagic-carbonate covered terraces linked by steeper intervals that expose chalk, semi-consolidated talus and basement rocks (basalts and serpentinized ultramafics).

The topography of the terraces is complex; at a regional scale the platforms, which vary in width from one hundred meters to over a thousand meters, dip gently

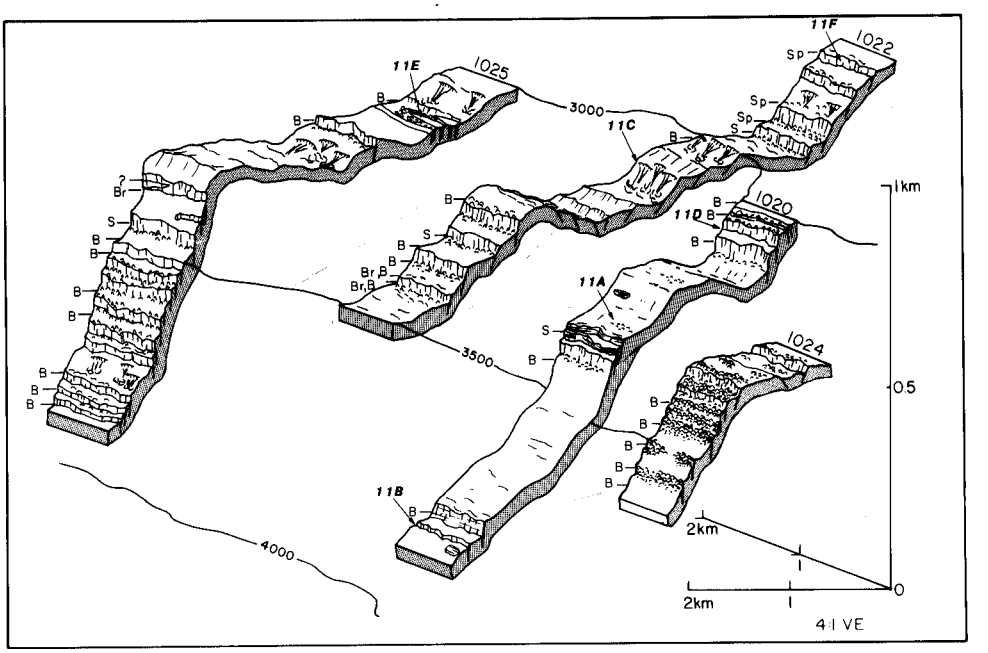

Fig. 10. Geologic reconstructions (as in Figure 7) of ALVIN dives 1020, 1022, 1024, and 1025. Letters S (sediment), B (basalt) and Sp (serpentinite) indicate locations of samples collected along the dive traverses, talus is indicated by discontinuous black lines; sediment patches shown as white areas; vertical dikes (only at end of dive 1025) are indicated by double lines; fault scarps are depicted as steep lines but dip of faults is hypothetical. Depth in m.

(5° to 10°) towards the rift axis. In some places the platforms are incised by broad open depressions bounded by steep slopes (~50°) that strike perpendicular to the local contours and that develop several meters of relief. The sides of these valleys are cut by steep-sided erosional gullies that terminate along the axis of the depression, which are littered with fragments of chalk and ferromanganese encrusted igneous rock fragments. Chalk and semi-consolidated talus outcrop on the flanks of the channels and we interpret them to be erosional in origin, serving as pathways for the downslope migration of debris shed from unstable slopes found higher up the rift wall.

Superimposed upon the gently dipping carbonate and talus-covered platforms is a complexly arranged series of ridges and troughs with relief of several meters. Given the limited perspective provided by the submersible, it is difficult to establish whether or not this hummocky terrain develops a systematic grain across and along the predominantly NE–SW strike of the platforms. We suspect that the undulating fabric is the product of two different but complimentary processes. Volcanic constructional terrain that has been passively rafted up and away from the axis of accretion and that is now overlain by a variable thickness of sediment almost certainly constitutes bedrock beneath the terraces and is responsible for some of the relief, albeit muted, now observed at the seafloor. This signal, however, is degraded and perhaps completely lost in many instances by the development of thick, lobate talus wedges that form at the base of steep escarpments and that coalesce along strike, prograding out across the volcanic terrain. The development and growth of talus deposits is vigorous when the seafloor is young and escarpments are steep, but by the time these parcels of seafloor reach intermediate levels along the rift walls, broad expanses have been buried beneath rubble and are apparently left unaffected by further faulting.

The monotony of the sediment-covered platforms is broken intermittently by relatively narrow, southward-facing, steep intervals that are sites where recent faulting has taken place, mass wasting is still active, and bedrock or semiconsolidated sediment is exposed. The relief produced by these topographic steps is variable. In some cases these intervals represent small shoulders of rubble a few meters high protruding through the pelagic blanket (Figure 11a), but in other instances the slopes approach near vertical and several tens of meters of rugged relief are observed. On the escarpment faces, three units occur: igneous rocks; welded talus comprised of igneous rocks and a carbonate matrix; and laminated chalk. These indicate the complex interplay between igneous processes, mass wasting and pelagic sedimentation that must have occurred during the initial phase of sea floor accretion. At the base of the precipitous intervals fresh, sediment-free rubble, composed of a mixture of the rock types exposed on the escarpments above, are observed to create ramps (up to 30° slopes) that abut the steep scarps. The intervals of large relief (>20 m) demarcate zones a few hundred meters wide, composed of several closely-spaced escarpments linked by narrow bands of talus.

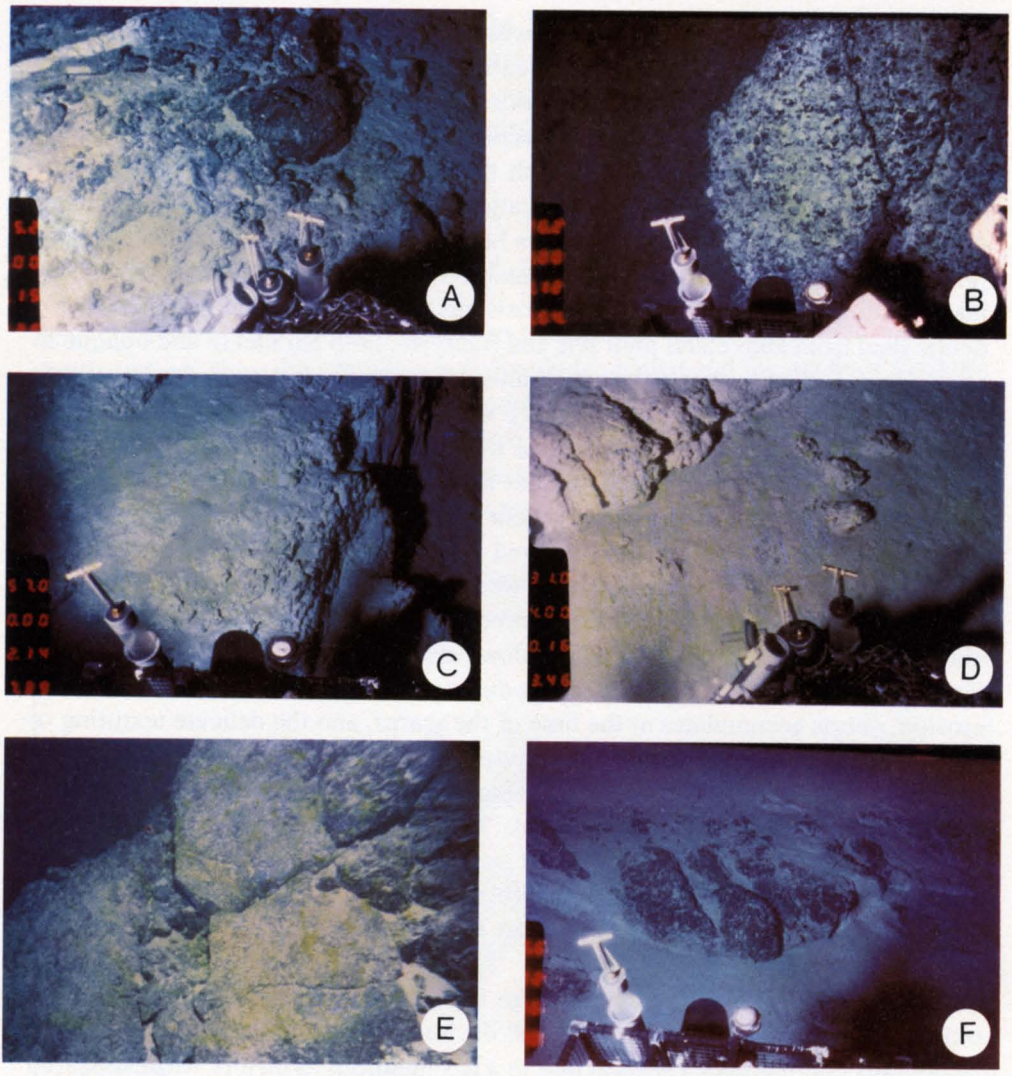

Fig. 11. Photographs of western rift valley wall. (A) Small outcrop of rubble (degraded scarp?) that is cut by a very fresh scarplet, only a few centimeters high (scarp face is white area at upper left), that strikes NE–SW. Field of view is about 3.0 m wide. (Hull-mounted camera, ALVIN dive 1020; time 15:09:26; depth 3292 m; see Figure 10 for location). (B) Near vertical wall of semiconsolidated rubble (igneous cobbles in a carbonate maxtrix); wall strikes NE–SW and has relief of approximately 10 m. Field of view is about 3.0 m wide. (Hull-mounted camera, ALVIN dive 1022; time 12:05:54; depth 3360 m; see Figure 10 for location). (C) Near vertical, 1.0 m high, fault scarp that cuts semiconsolidated carbonate and strikes E–W; note vertical striae and crooked trace indicating dip-slip motion. Field of view is about 3.0 m wide. (Hull-mounted camera, ALVIN dive 1022; time 14:37:39; depth 3052 m; see Figure 10 for location). (D) Degraded and eroded scarp that cuts semiconsolidated carbonate; scarp strikes N–S. Field of view is about 3.0 m wide. (Hull-mounted camera, ALVIN dive 1020; time 16:53:46; depth 3098 m; see Figure 10 for location). (E) Exposure of fractured basalt cut by massive basaltic dikes, about 0.5 m wide, standing near vertical and striking NNW–SSE (J. Karson, hand-held photo, ALVIN dive 1025; depth 3310 m; see Figure 10 for location). (F) Highly degraded outcrop (fault scarp?) of serpentinized ultramafic rock. Field of view is about 4.0 m wide. (Hull-mounted camera, ALVIN dive 1022; time 16:50:38; depth 2731 m; see Figure 10 for location).

Most of the escarpments high on the west wall look relict: the outcropping rock has been badly degraded by erosion creating relatively low slopes, and the talus strewn at the base of the scarp is imbedded in a matrix of pelagic sediment with exposed rocks serving as pedestals for sessile organisms. This sense of tranquility and slow decay contrasts markedly with those areas which exhibit evidence for active slope development and modification. In several instances we observed near-vertical scarps a few tens of meters high that expose semi-consolidated talus (Figures 10, 11b). These scarps are unstable and are being actively modified by mass wasting: narrow gorges and channels indent the scarp creating channels for debris shed from above;and joint sets and fractures, both parallel to and oblique to scarp faces, isolate large blocks which must periodically peel away from the cliff. Such terrain is clearly evolving rapidly and the relief developed in the semi-consolidated talus and the resultant mass wasting is certainly a product of episodic and recent uplift of underlying basement along inward-facing faults.

The most definitive evidence for recent faulting is the existence of small (6 to 50 cm), near-vertical scarps, encountered at several isolated localities along the west wall, that expose pervasively burrowed and poorly bedded semi-consolidated carbonate. Some scarps must be very recent because their faces are angular, with abundant striae-like grooves trending down-dip, and the bases of the scarps are free of talus (Figure 11c). Older scarps cutting carbonate have been rounded by erosion; debris accumulates at the base of the scarps, and the delicate texturing of the fault faces is no longer apparent (Figure 11d). These small scarps tend to occur in closely spaced groups a few meters apart and could be traced along strike for only a short distance (several meters). These faults disrupting the semi-consolidated carbonate blanket probably reflect deformation of the underlying basement. A few of them have a northerly ridge axis-parallel trend, but the majority strike approximately parallel to the regional morphologic grain of the western rift-valley wall (070°).

The numerous well-defined fault scarps that cut igneous basement have heights of less than 0.5 m to more than 10 m and the larger-relief scarps were observed to be laterally continuous for several tens to a few hundreds of meters. Most appeared to be fairly linear on side-scanning sonar records, but direct observations showed many to be incised by narrow steep-sided gullies indicating modification by mass wasting. The escarpments tend to occur in close proximity to one another and large fault scarps are often accompanied by a family of several smaller parallel scarps within a few tens of meters. The orientations of fault scarps and well-defined reflectors recognized on the ALVIN sonar system for the west wall range from 350° through 000° to 090° (Figure 8). Trends of 000° to 030° are dominant along the northern traverses (Dives 1020 and 1024) but, with increasing proximity to the transform, trends ranging from 035° to 090° are the more commonly observed (Dives 1022 and 1025). There also appears to be some tendency for scarps closer to the transform and at greater depths to have a more E–W orientation, but escarpments higher on the slope have dominantly oblique trends (030° to 060°).

Most of the scarps that we observed are sufficiently small in terms of relief and continuity along strike that they would be difficult to detect by investigative instruments located at or near the sea surface (i.e. Sea Beam, GLORIA). The structural features observed during ALVIN and ANGUS traverses are the individual components of a larger morphologic ensemble that is characterized by the temporal and spatial integration of faulting and mass wasting. Based on near-bottom observations it is clear that N–S and, to a lesser extent, NE–SW and E–W striking faults are all important in contributing to the structural fabric of the western wall (Figure 8). Inspection of the bathymetric map (Figure 2), however, indicates that at this scale the morphology of the western wall is dominated by laterally-continuous, inwardly-facing lineaments that strike NE–SW and the evidence for the development of structures that strike N–S and E–W is largely lost. We suggest that the strong oblique signal in the bathymetric map is not solely controlled structurally but is partially the product of mass wasting which has obscured the westward-stepping topographic fabric created by N–S and E–W trending faults through the development of the steep-sided (20° to 60°) talus wedges that coalesce along strike muting and modifying the structural grain of the basement. The topographic illusion created at a regional scale is that oblique trending faults could be the sole relief-producing structures.

The vertical relief of the fault scarps observed on the western rift valley wall indicates that at least some component of dip-slip motion has occurred, and we have no evidence to suggest any significant oblique-slip or strike-slip motions. Serrated surface traces comprised of short (<1 m) linear segments, and vertical slickensides, striae, and grooves all document, for example, that the most recent motion was dip-slip. Although it is possible that we observed only the results of some comparatively recent dip-slip motion on faults with complex displacement histories, it is significant that there was no evidence, even on those faults with an E–W, transform-parallel strike, to suggest anything but dip-slip faulting. It is interesting to note that the young-looking fault scarps of the western wall occur in the region that was found to be the most seismically active part of this ridge-transform intersection during a microseismicity investigation (Rowlett, 1981). The distribution of microearthquake epicenters define a swath that is coincident with the oblique trending western wall of the rift valley.

A diverse suite of lithologies outcrop on the escarpments of the western wall. In the depth range of 2500 to 4000 m we sampled variably indurated chalks, basaltic rocks and serpentinite (serpentinized ultramafics). The chalks included both low density plastic types as well as denser, harder varieties (Karson and Kidd, in preparation). The basaltic rocks are encrusted with a thin veneer of ferro-manganese oxide (a few millimeters to one centimeter) and are devoid of the glassy surfaces or delicate ornamentation that is characteristic of very fresh extrusive basalts. At the end of Dive 1025, a large outcrop (at least 50 by 30 m) of slightly fractured pillow lavas was observed. Its undulating upper surface is bounded by steep scarps trending along and across the slope exposing a family of at least three

subparallel subvertical dikes that cut the pillow lavas (Figure 11e). The dikes are 0.5 to 1 m in width, have sharp contacts with the intervening lavas, strike 050° to 070° and are spaced about 0.5 to 3 m apart. These dikes suggest that at least some extension takes place across the oblique structural trends defined in the area. They have the wrong orientation to have been rotated from an initial ridge-parallel orientation by shearing across the transform domain (Tchalenko, 1970).

At the end of Dive 1022, which reached the shallowest levels investigated along the western wall, serpentinized ultramafic rocks were sampled at four different localities over a distance of 700 m. These samples were collected from relatively small scarps less than a few meters high or from talus at the base of outcrops. The serpentinites are variably altered, intensely weathered and cut by numerous anastomosing shear zones spaced at intervals of a few millimeters to about 1cm. The exposures of serpentinite do not create well-defined scarps, in contrast to other basement outcrops, but rather consist of low ridges that lack a strong preferred orientation (Figure 11f). The outcrops of serpentinite are separated by smooth, gently sloping carbonate-covered terraces. At one locality near an outcrop of serpentinite the carbonate blanket is disrupted by several small (tens of centimeters) near-vertical scarps. Bathymetric data indicate that this portion of the west wall is characterized by terrain that lacks a well-defined topographic grain, exhibiting a dome and basin morphology.

3.4. The transform domain

ANGUS lowering 123 began in the relatively fresh volcanic constructional terrain along the axis of accretion and traversed southwards down into and across the flat sediment-covered floor of the nodal basin (Figures 2, 6). The traverse then ascended the steep, E–W striking south wall of the nodal basin and ended by tracing this wall westwards. These photographic data from ANGUS 123 provide some insights into the nature and location of the boundary between the axis of accretion and the Oceanographer Transform. Volcanic basement, degraded by mass wasting and disrupted by steep escarpments and fissures striking approximately parallel to the ridge axis, can be traced down into and along the northeastern flank of the nodal basin until the basaltic outcrops are lost beneath a smooth blanket of sediment. Fissures that strike N–S, and collapse pits disrupt the sediments on the northern side of the nodal basin, but within the basin the sediment surface along the track is smooth except for one outcrop of hard-rock rubble.

Seismic reflection data indicate that the basin is floored with approximately 100 m of sedimentary material (Schroeder, 1977) and the relatively high rates of sedimentation that can be inferred from such a thick sedimentary cover on young crust suggests that all but the most recent evidence of tectonics will be obscured by sediments funneled into the depression. The nodal basin is a depositional center for debris flows and turbidity currents shed from high surrounding terrain. Fine-grained sediments transported by geostrophic currents that cross the MAR following the transform valley will tend to be deposited in this region as the

currents lose competence spreading out across the broad triangular basin. Given the relatively thick sedimentary overburden, the axis of accretion could lie beneath the sediment blanket with basalts intruding into the sediments of the nodal basin; a situation similar to the accretionary environment known to characterize the Guymas Basin in the Gulf of California (DSDP drilling results Leg 64). Alternatively, it is possible that the zone of most recent volcanism lies along the eastern side of the nodal basin. We have no data here but this geometry would be similar to the Kane Fracture Zone (Karson and Dick, 1983).

The southern side of the nodal basin is defined by a WNW–ESE trending slope that develops over 1000 m of relief (Figures 2, 6). Towards the west, over a distance of 15 km, the nodal basin shallows and narrows as the E–W trending southern escarpment merges with the NE–SW striking western flank of the nodal basin to form the narrow 2 to 3 km wide floor of the Oceanographer Transform. Two crossings of the south wall and two crossings of the western end of the nodal basin indicate that large portions of the southern flank of the nodal basin are characterized by smooth, sediment-covered slopes that dip down towards the floor of the nodal basin. Current indicators are rare along the rift valley but along portions of the south slope the sediments are sculptured by bottom currents as evidenced by cuspate ripples, furrows and troughs, and long parallel ridges.

Along each of the four crossings of the flanks of the nodal basin there is evidence of active mass wasting (Figures 6, 8). The steep slope segments are in places parallel to regional contours and face towards the floor of the nodal basin but, in other cases, the escarpments depart markedly from regional trends resulting in complex microtopography. In all cases, narrow rills and gullies scar the face of the scarps and loose blocks of consolidated sediment and rocks litter the gullies and accumulate at the base of the slopes. Fissures, oriented approximately parallel to contours, are associated with the steep intervals. These zones of active erosion are distributed along an E–W trending swath that is about two kilometers wide and that is aligned, when extrapolated along strike to the west, with the axis of maximum depth of the Oceanographer Transform. Some tens of kilometers to the west our investigation of the Oceanographer Transform (OTTER, in prep.) yielded evidence for recent tectonism along the transform valley that is concentrated along a 2 km-wide, E–W trending zone centered about the axis of maximum depth. The narrow E–W trending zone of inferred recent faulting along the southern flank of the nodal basin may therefore represent the location of the principal transform displacement zone.

The orientations of the few scarps observed along the southern flank of the nodal basin (Figure 8) do not appear to be related to any systematic family of lineaments that might be related to the nucleation and development of a shear zone along the PTDZ (e.g. Reidel, 1929; Tchalenko, 1970). It is possible that such a fracture or lineament pattern may exist at depth, but such features may not be faithfully transmitted to the surface due to the mechanical properties of the sediment and rubble above the basement. The valley fill could deform by slumping, block

rotation, block-boundary sliding, and jostling of this inhomogeneous assemblage rather than by the formation of discrete fault planes. This style of deformation may result in only locally well-defined surface scarps and more generally in broad ridges and basins related to differential uplift and sagging of the valley fill.

4. Summary and Interpretation

The geology of the morphotectonic elements comprising the eastern ridge-transform intersection of the Oceanographer Transform sheds light on a few questions that have recently been addressed in the literature. In the following sections we comment on some of these points and emphasize the significance of our observations.

4.1. Crustal thinning near the Oceanographer fracture zone

There is growing evidence that the thickness and properties of oceanic crust created at and proximal to ridge-transform-ridge intersections may be anomalous compared to crust created farther from this kind of plate boundary. In order to explain the recovery by dredging of gabbroic rocks from high levels on transform valley walls, Francheteau *et al.* (1976) suggested that the shallow intrusive and extrusive carapace exposed on the walls of transform valleys may be thinner than normal. The abundant recovery by submersible ALVIN of gabbroic and ultramafic rocks from small throw faults that bound the rift valley of the 80 km long Mid-Cayman Rise spreading center lead investigators to propose that the crust created proximal to slowly-slipping ridge-transform boundaries is anomalously thin (Fox, 1978; CAYTROUGH, 1979; Stroup and Fox, 1981). A seismic refraction experiment in and around the Kane Fracture Zone showed that upper mantle velocities exist at very shallow levels (2 km) within the fracture zone domain (Detrick and Purdy, 1980; Fox *et al.*, 1980). The apparent anomalous crustal thickness associated with ridge-transform intersections suggested that the truncating cold edge of the transform fault cools the wedge of asthenosphere rising beneath the axis of accretion proximal to the transform (Sleep and Biehler, 1970) resulting in the production of less basaltic melt per unit time and leading to thinner crust (Gallo and Fox, 1979; Stroup and Fox, 1981; Fox *et al.*, 1980; Fox and Gallo, 1984). Recent field investigations of the eastern intersection of the Kane Transform with the Mid-Atlantic Ridge by submersible ALVIN (Karson *et al.*, 1980; Karson and Dick, 1983), seismic refraction investigations of the VEMA Transform (Detrick *et al.*, 1982) and the Oceanographer Transform (Sinha and Louden, 1983) all support the notion that the oceanic crust is anomalously thin along and proximal to these transform faults.

Our field data from the eastern intersection of the Oceanographer Transform and the Mid-Atlantic Ridge are consistent with the thin crust hypothesis (Figure 12). The recovery of serpentinized harzburgites, representative of the deepest units exposed in ophiolites, from localities high up on the western rift valley wall is suggestive that the crust is very thin or even discontinuous in this region. The

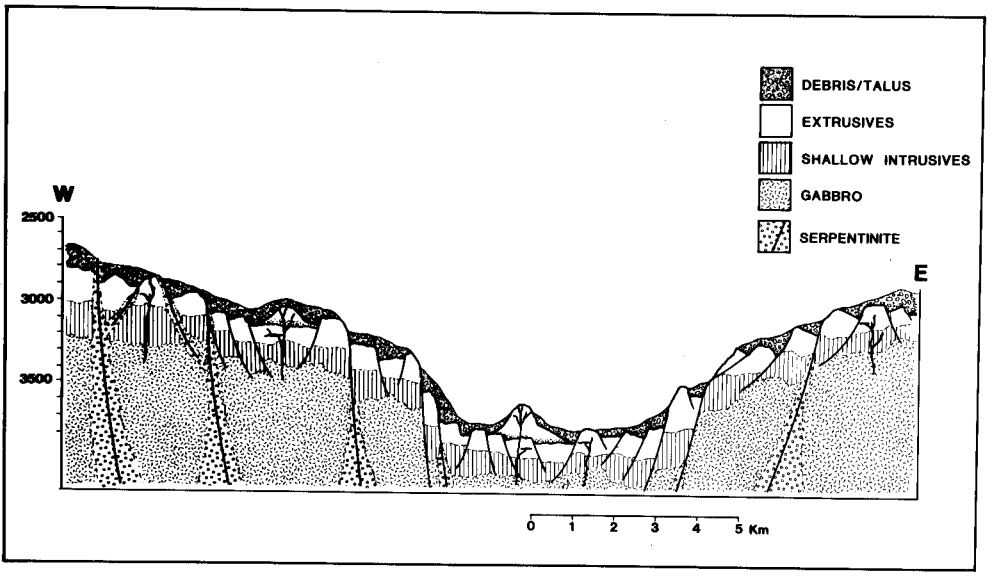

Fig. 12. Simplified east-west geologic cross-section across the rift valley just north of the Oceanographer Transform (see Figure 8 for location). The diagram suggests two generations of faults. The first family of faults form in the extensional tectonic environment that characterizes the rift valley floor. These faults are numerous, they becaome listric at relatively shallow crustal levels (base of the shallow intrusives), and they disrupt the igneous stratigraphy created by accretion. The second family of faults form at the edges of the rift valley floor, extend to the base of the lithosphere, and bound blocks of crust of variable width. It is motion along these faults that create the step-like topography of the rift-valley wall. The magmatic componet of the crust proximal to the ridge-transform boundary is thin making it easy for seawater to percolate along these faults and to hydrate upper mantle rocks. The hydrated products, serpentinites, rise diapirically along the faults intruding the oceanic crust. Thickness of debris/talus blanket exaggerated for clarity; the vertical lines symbolizing the shallow intrusives do not indicate the orientation of dikes within blocks; complex, intrusive and extrusive relationships within the shallow levels of the oceanic crust are not shown.

serpentinites were sampled from small scarps that develop relief of only several meters above the surrounding sediment-covered terrain indicating that structural thinning of the crustal section by faulting was not a major factor in the exposure of these rocks. Assuming that all crust in this area moves laterally away from the ridge axis along a flow line parallel to the transform at a half spreading rate of 1.5 cm yr^{-1}, these serpentinites crop out in terrain approximately 0.5 my old.

Our sampling along and up the western rift walls is not so dense that we can accurately assess the distribution and arrangement in space of the major rock types. During our field program we recovered extrusive basalt, intrusive basalt and serpentinized ultramafics. Although no gabbroic rocks were recovered we predict they are likely to be exposed at some localities on the rift walls. It is not clear whether or not the serpentinites are in place having been exposed by erosion or whether they have risen diapirically to shallower structural levels along faults. It is possible that progressive erosion of any particular crustal packet, as it is elevated out of the

ridge-transform intersection deep, leads to the exposure of the plutonic and ultramafic rocks through erosion of the thin basalt cover. The shearing foliation observed in some ultramafic samples would be a product of faulting. The distribution of observed basaltic outcrops largely at greater depths on the western slope of the intersection depression is consistent with this hypothesis. Alternatively, if the crust is very thin (<2 km) proximal to the ridge-transform environment as indicated by geological (CAYTROUGH, 1979; OTTER, 1980; Stroup and Fox, 1981; Karson *et al.*, 1980; Karson and Dick, 1983) and geophysical evidence (Detrick and Purdy, 1980; Sinha and Louden, 1981; Detrick *et al.*, 1982) then it would be relatively easy for sea water to follow fault-produced permeable pathways to depth and hydrate relatively young, hot ultramafic rocks; the hydrated product, serpentinite, would then rise along faults as narrow screens or as a diapir shouldering its way up and through the young crust (Figure 12). Serpentinization models of this kind have been discussed by various authors (Aumento and Loubat, 1971; Bonatti, 1976; 1978; Francis, 1981), but these models involved normal thickness of oceanic crust (5–7 km). Given the young age of the lithosphere and the rheology of serpentinite (Raleigh and Patterson, 1965; Dengo and Logan, 1981), we suspect that the serpentinite sampled from the outcrops high on the rift valley walls has not migrated upward more than a few hundred meters. This motion would be facilitated by pronounced weakening of peridotite during hydration/dehydration reactions (Raleigh and Patterson, 1965). The complex fabrics and amphibole-bearing hydrothermal veins in these serpentinites bear witness to a complex history of deformation, hydration and possibly dehydration events that probably diminish rapidly as the lithosphere ages and cools moving away from the ridge axis.

Serpentinite bodies have been observed in ophiolites, especially in association with a transform fault setting (e.g. Moores and Vine, 1971; deWit *et al.*, 1978; Karson *et al.*, 1983) and these bodies seem to be of the same general size as the dome-like structures we observe on the western median valley wall. The thin or even discontinuous mafic material and abundant serpentinites of the western wall will pass laterally along the north flank of the Oceanographer Transform where they could evolve into an anomalously shallow serpentinite ridge through continued hydration and diapiric rise of ultramafic rocks. Shallow transform ridges are known to be characteristic of some slowly-slipping ridge-transform-ridge plate boundaries (Bonatti and Honnorez, 1976; Sclater *et al.*, 1978) and these serpentinite ridges may have their origin proximal to ridge-transform intersections where thin crust is disrupted by numerous faults that allow water to penetrate down to the ultramafic rocks.

The reconstruction of pre-hydration phase assemblages of some of the ultramafic rocks from the escarpments that flank the Oceanographer Transform indicate that the igneous phases equilibrated in the spinel peridotite facies (plagioclase appears to be absent or minor; Bonatti and Hamlyn, in preparation). This implies pressures during crystallization of approximately 8 to >9 K bars, corresponding to depths in excess of 30 km below the sea floor. Similar depths of crystallization have been

suggested for ultramafic rocks recovered from other transform faults (Bonatti and Hamlyn, 1978; Hamlyn and Bonatti, 1980). In the absence of any evidence suggesting tectonic uplift of these upper mantle rocks over vertical distances of 20 km, it seems likely that the mineral phases of the serpentinized ultramafic rocks from the Oceanographer area crystallize at depth and then are passively transported to the near surface on a rising limb of the asthenosphere beneath the ridge axis (Elthon *et al.*, 1982).

4.2. Ridge-transform coupling

Several geophysical studies of ridge-transform intersections have documented the existence of lineaments with trends that are oblique to both the strike of the transform and the adjoining ridge segments (Crane, 1976; Whitmarsh and Laughton, 1977; Lonsdale, 1978; Searle, 1979; Macdonald *et al.*, 1979). The significance of these lineaments has been interpreted in different ways. Studies of continental shear zones and clay box experiments have demonstrated the formation and evolution of certain structures that accommodate strike-slip displacement during the initial stage of shear zone development (e.g. Tchalenko, 1970; Tchalenko and Ambraseys, 1972; Wilcox *et al.*, 1973). It has been suggested that these oblique trending structures represent shear fractures, known as Reidels and anti-Reidels, that form proximal to the transform boundary during the initial stages of formation of the shear zone (Courtillot *et al.*, 1974). Such a model predicts that the oblique structures accommodate a component of strike-slip motion, assumes that plane strain applies to the deformation, and considers only the first (infinitesimal) increment of strain without regard to subsequent increments.

Another model suggests that the tensional state of stress along the accreting plate boundary is distorted by a shear-couple located at the ridge-transform boundary (Crane, 1976; Searle and Laughton, 1977; Lonsdale, 1978; Searle, 1979). A prediction of this model is that the oblique-trending faults would be solely a product of dip-slip motion. Direct measurements of oblique trending faults at the Tamayo Transform – EPR intersection (Tamayo Scientific Team, 1983) and Kane Fracture Zone – MAR Intersection (Karson and Dick, 1983) demonstrate that no significant strike-slip motion has occurred on these faults. The shear couple responsible for this distortion is not a shallow level effect, but rather one generated primarily at depth through the welding of the upwelling asthenospheric material beneath the ridge axis to the cold opposing boundary wall. The stronger this weld becomes, the greater the magnitude of the shear stress transmitted along the ridge axis (Gallo *et al.*, 1980; Tamayo Scientific Team, 1983; Fox and Gallo, 1984). The result is the progressive reorientation of the minimum compressive stress axis from normal to the ridge, at some distance from the ridge-transform intersection, to an oblique angle near the transform boundary. This model predicts extensional tectonics and volcanism about an axis that intersects the transform at a variable angle that is less than 90° and that the angle will depend on the magnitude of the

shear couple relative to ridge-normal extension.

Our investigations of structures developed along the floor of the rift valley and on the western rift valley wall (Figure 8) support this shear couple model. We have documented only normal (dip-slip) faulting on the oblique structures as well as on transform and ridge axis parallel structures. Additional evidence of extension across the oblique western wall of the OFZ area includes open fissures, fissure eruption ridges, and dikes oriented parallel to this oblique trend (Figure 8). The observations constrain the location of the present PTDZ to an extremely narrow zone (<2 km wide) in the transform valley (OTTER, in prep.).

4.3. Temporal evolution of the ridge-transform intersection

Recent comparative studies of different segments of the Mid-Atlantic Ridge show that they are distinctly different in their first-order morphologies and tectonic properties (Atwater, 1979; Crane and Ballard, 1981). The FAMOUS area's Narrowgate Rift is only a few kilometers wide and is marked by large, only slightly disrupted central volcanoes (e.g. Mt. Pluto, Mt. Venus, etc.). In contrast, the AMAR Rift just to the south of the FAMOUS area is a 30 km-wide flat-floored median valley that lacks the young-looking volcanic features of the Narrowgate Area and is dissected by numerous faults. These two areas are believed to represent different parts of the cycles of tectonic extension and episodic volcanism (Atwater, 1979; Crane and Ballard, 1981). If such cyclic behavior characterizes ridge segments away from major transform faults a similar pattern of events might be expected proximal to ridge-transform intersections. If the overall, time-averaged magmatic budget is limited near these slowly-slipping plate boundaries as suggested by Gallo and Fox (1980) and indicated by the relatively thin volcanic unit near transforms (Francheteau *et al.*, 1976; CAYTROUGH, 1979; Stroup and Fox, 1981; Karson *et al.*, 1980; Karson and Dick, 1983), tectonic activity may dominate there regardless of processes further away from the ridge-transform intersections. Our observations at the OFZ area clearly show that in this area tectonic activity is much more important than volcanism, at least at present. At the Kane Transform, however, (Karson *et al.*, 1980; Karson and Dick, 1983) relatively young volcanic constructional ridges can be traced down the two rift axes and across the nodal basins. If these two morphotectonic forms represent endpoints of cyclic behavior that characterize ridge-transform intersections, volcanic or tectonic activity may be relayed from one ridge segment to the next by episodic slip along intervening transforms (Karson and Dick, 1983). Time-dependent anelastic deformation of the lithosphere along transforms could impose time delays at each transform as the propagation of an extensional event proceeds down a ridge system.

Acknowledgements

The authors wish to thank the officers and crew of the R/V KNORR and R/V

LULU and the members of the ALVIN submersible team for their help during the field program; without their assistance, dedication and expertise this project would not have been possible. We thank Drs K. Louden and J. Peirce for their constructive comments made during the review process. Grants from the Office of Naval Research supported the field work and the data analysis and is gratefully acknowledged; the following grants supported the program: N-0014-80-C-0287 (P.J.F., J.A.K., H.S., W.S.F.K., J.B.S., D.J.F., D.G.G.); N-00014-81-C-0820 (P.J.F., H.S., D.G.G.); N-00014-80-C-098-S.W. (K.C.); N-00014-80-C-0098-S.T. (E.B., P.H.). WHOI contribution number 5351.

References

Atwater, T.: 1979, 'Constraints from the FAMOUS Area Concerning the Structure of the Oceanic Section', in Talwani, M., Harrison, C. G., and Hayes, D. E. (eds.), *Deep Drilling Results in the Atlantic Ocean: Ocean Crust 2nd Maurice Ewing Memorial Symp., Amer. Geophys. Union* **2**, 33–42.

Aumento, F. and Loubat H.: 1971, 'The Mid-Atlantic Ridge near 45° N, XVI Serpentinized Ultramafic Intrusions', *Can. Jour. Earth Sci.* **8**, 631–663.

Ballard, R. and van Andel, T. H.: 1977, 'Morphology and Tectonics of the Inner Rift Valley at Latitude 36° 50′ N on the Mid-Atlantic Ridge', *Geol. Soc. Amer. Bull.* **88**, 507–530.

Ballard, R., Francheteau, J., Juteau, T., Rangin, C., and Normark, W.: 1980, 'East Pacific Rise at 21° N: The Volcanic, Tectonic, and Hydrothermal Processes of the Central Axis', *Earth and Planet. Sci. Letters* **55**, 1–10.

Bonatti, E.: 1976, 'Serpentinite Protrusions in the Oceanic Crust', *Earth and Planet. Sci. Letters* **32**, 107–113.

Bonatti, E.: 1978, 'Vertical Tectonism in Oceanic Fracture Zones', *Earth and Planet. Sci. Letters* **37**, 369–379.

Bonatti, E. and Hamlyn, P. R.: 1978, 'Mantle Uplifted in the Western Indian Ocean', *Science* **201**, 249–251.

Bonatti, E. and Honnorez, J.: 1976, 'Sections of the Earth's Crust in the Equatorial Atlantic', *J. Geophys. Res.* **81**, 4104–4116.

CAYTROUGH: 1979, 'Geological and Geophysical Investigations of the Mid-Cayman Spreading Center: Initial Results and Observations', in Talwani, M., Harrison, C. G., and Hayes, D. E. (eds.), *Deep Drilling Results in the Atlantic Ocean: Ocean Crust, 2nd Maurice Ewing Memorial Symp., Amer. Geophys. Union* **2**, 66–93.

Courtillot, V., Tapponier, P., and Varet, J.: 1974, 'Surface Features Associated with Transform Faults: A Comparison between Observed Examples and Experimental Models', *Tectonophysics* **24**, 317–329.

Crane, K.: 1976, 'The Intersection of the Siquieros Transform Fault and the East Pacific Rise', *Marine Geology* **21**, 25–46.

Crane, K. and Ballard, R.: 1981, 'Volcanics and Structure of the FAMOUS Narrowgate Rift: Evidence for Cyclic Evolution', *J. Geophys. Res.* **86**, 5112–5124.

CYAMEX Scientific Team: 1981, 'First Manned Submersible Dives on the East Pacific Rise at 21° N (Project RITA): General Results', *Mar. Geophys. Res.* **4**, 345–379.

Dengo, C. A. and Logan, J. M.: 1981, 'Implications of the Mechanical and Frictional Behavior of Serpentinite to Seismogenic Faulting', *J. Geophys. Res.* **86**, 10771–10782.

Detrick, R. S., Cormier, M. N., Prince, R. A., and Forsyth, D. W.: 1982, 'Seismic Constraints on the Crustal Structure Within the VEMA Fracture Zone', *J. Geophys. Res.* **87**, 10, 599–10, 612.

Detrick, R. S. and Purdy, G. M.: 1980, 'The Crustal Structure of the Kane Fracture Zone from Seismic Refraction Studies', *J. Geophys. Res.* **85**, 3759–3777.

deWit, M. J., Dutch, S., Kligfield, R., Allen, R., and Stern, C.: 1977, 'Deformation, Serpentinization, and Emplacement of a Dunite Complex, Gibbs Island, South Shetland Islands: Possible Fracture Zone Tectonics', *J. Geol.* **85**, 745–762.

Dick, H. J. B.: 1977, 'Partial melting in the Josephine Peridotite I: The Effect on Mineral Composition and its Consequences for Geobarometry and Geothermometry', *Amer. J. of Sci.* **227**, 801–832.

Elthon, D., Casey, J., Casey, G. F., and Komer, S.: 1982, 'Mineral Chemistry of Ultramafic Cumulates From the North Arm Mountain Massif of the Bay of Islands Ophiolite: Evidence for High-Pressure Crystal Fractionation of Oceanic Basalts', *J. Geophys. Res.* **87**, 8717–8734.

Fox, P. J.: 1978, 'The Effect of Transform Faults on the Character of the Oceanic Crust', *Geol. Soc. Amer. Abs. with Prog.* **7**, 403.

Fox, P. J., Detrick, R. S., and Purdy, G. M.: 1980. 'Evidence for Crustal Thinning near Fracture Zones: Implications for Ophiolites', in Panayiotou, A. (ed.), *Proceedings of the International Ophiolite Symp. Cyprus*, Geol. Surv. Dept. 161–168.

Fox, P. J. and Gallo, D. G.: 1984, 'A Tectonic Model for Ridge-Transform-Ridge Plate Boundaries: Implications for the Structure of the Lithosphere', *Tectonophysics* **104** (in press).

Fox, P. J., Lowrie, A., and Heezen, B. C.: 1969, 'Oceanographer Fracture Zone', *Deep-Sea Res.* **16**, 55–66.

Fox, P. J., Schreiber, E., Rowlett, H., and McCamy, K.: 1976, 'The Geology of the Oceanographer Fracture Zone: A Model for Fracture Zones', *J. Geophys. Res.* **81**, 4117–4128.

Fox, P. J., Schroeder, F., Moody, R. M., and Pitman, W. C., III: 1983, 'The Morphotectonic Character of the Oceanographer Fracture Zone', *Mar. Geophys. Res.* (under review.)

Francheteau, J., Choukroune, P., Hekinian, R., LePichon, X., and Needham, D.: 1976, 'Oceanic Fracture Zones do not Provide Deep Sections into the Crust', *Can. J. Earth Sci.* **13.**, 1223–1235.

Francis, T. G.: 1981, 'Serpentinization Faults and their Role in the Tectonics of Slow-Spreading Ridges', *J. Geophys. Res.* **86**, 11616–11622.

Gallo, D. G. and Fox, P. J.: 1979, 'The Thermo-Evolution of Oceanic Crust and Lithosphere Proximal to Transform Boundaries', *Geol. Soc. Amer., Abs. with Progs.* **11**, 429.

Gallo, D. G., Rosencrantz, E. R., and Rowley, D. B.: 1980, 'Oblique Structures at Ridge-Transform Intersections: Implications for Ridge Dynamics and Pole Determinations', *Trans. Amer. Geophys. Union EOS* **61**, 358.

Hamlyn, P. R. and Bonatti, E.: 1980, 'Petrology of Mantle-Derived Ultramafics from the Owen F.Z., NW Indian Ocean: Implications for the Nature of Oceanic Upper Mantle', *Earth Planet. Sci. Letters* **48**, 65–79.

Karson, J. and Dewey, J.: 1978, 'Coastal Complex, Western Newfoundland, an Early Ordovician Oceanic Fracture Zone', *Geol. Soc. Amer. Bull.* **89**, 1037–1049.

Karson, J. and Dick, H.: 1983, 'Tectonics of Ridge-Transform Intersections at the Kane Fracture Zone', *Mar. Geophys. Res.* **6**, 51–98.

Karson, J. Dick, H. J. B., Bryan, W. B., and Thompson, G. A.: 1980, 'Tectonics of Ridge-Transform Intersections at the Kane Fracture Zone', *Geol. Soc. Amer., Abs. with Progs.* **12**, 458.

Karson, J., Elthon, D. E., and DeLong, S. E.: 1983, 'Ultramafic Intrusions in the Lewis Hills Massif, Bay of Islands Ophiolite Complex, Newfoundland: Implications for Igneous Processes at Oceanic Fracture Zones', *Geol. Soc. Amer. Bull.* **94**, 15–29.

Karson, J. and Kidd, W.: 'Cleavage in Chalks from the Oceanographer Fracture Zone', (in prep.)

Lonsdale, P.: 1978, 'Near-bottom Reconnaissance of a Fast-Slipping Transform Fault Zone at the Pacific-Nazca Plate Boundary', *J. Geol.* **86**, 451–472.

Macdonald, K. C., Kastens, K., Miller, S., and Spiess, F. N.: 1979, 'Deep-Tow Studies of the Tamayo Transform Fault', *Mar. Geophys. Res.* **4**, 37–70.

Menard, H. W. and Atwater, T.: 1968, 'Changes in the Direction of Sea Floor Spreading', *Nature* **219**, 463–467.

Moores, E. M. and Vine, J. F.: 1971, 'The Troodos Massif, Cyprus and Other Ophiolites as Oceanic Crust: Evaluation and Implications', *Trans. Roy. Soc. London* **A268**, 443–466.

Otter Scientific Team: 1980, 'The Oceanographer Transform: Submersible and Deep-Towed Camera Investigations', *EOS* **60**, 1105.

OTTER Scientific Team: 'The Geology of the Oceanographer Transform: The Transform Domain', *Mar. Geophys. Res.* (in prep.)

Phillips, J. D. and Fleming, H. S.: 1978, 'Multi-Beam Sonar Study of the Mid-Atlantic Rift Valley, 36°–37° N: FAMOUS', *Geol. Soc. Amer. Map Series* **19**.

Phillips, J. D , Fleming, H. S., Feden, R. H., King, W. E., and Perry, R. K.: 1975, 'Aeromagnetic Study

of the Mid-Atlantic Ridge Near the Oceanographer Fracture Zone', *Geol. Soc. Amer. Bull.* **86**, 1348–1357.

Raleigh, C. B. and Patterson, M. S.: 1965, 'Experimental Deformation of Serpentinite and its Tectonic Implications', *J. Geophys. Res.* **76**, 3965–3985.

Reidel, W.: 1929, Zur Mechanik Geologischer Brucherscheinungen', *Centralbl. fur Mineral. Geol. of Pal.* **1929B**, 354–368.

RISE Project Group: 1980, 'East Pacific Rise: Hot Springs Geophysical Experiments', *Science* **207**, 1421–1433.

Rona, P. A.: 1980, 'TAG Hydrothermal Field: Mid-Atlantic Ridge Crest at Latitude 26° N', *J. Geol. Soc. London* **137**, 385–402.

Rowlett, H.: 1981, 'Seismicity at Intersections of Spreading Centers and Transform Faults', *J. Geophys. Res.* **86**, 3815–3820.

Schroeder, F. W.: 1977, 'A Geophysical Investigation of the Oceanographer Fracture Zone and the Mid-Atlantic Ridge in the Vicinity of 35° N', Ph.D. Diss. Columbia Univ., 450 pp.

Sclater, J. G., Dick, H., Norton, I. O., and Woodroffe, D.: 1978, 'Tectonic Structure and Petrology of the Antarctic Plate Boundary Near the Bouvet Triple Junction', *Earth and Planet. Sci. Letters* **37**, 393–400.

Searle, R. C.: 1979, 'Side-Scan Sonar Studies of North Atlantic Fracture Zones', *J. Geol. Soc. London* **136**, 283–293.

Searle, R. C. and Laughton, A. S.: 1977, 'Sonar Studies of the Mid-Atlantic Ridge and Kurchatov Fracture Zone', *J. Geophys. Res.* **82**, 5313–5328.

Sinha, M. C. and Louden, K. E.: 1983, 'The Oceanographer Fracture Zone: I Crustal Structure from Seismic Refraction Studies', *Geophys. J. Roy. Astron. Soc.*, **75**, 713–736.

Sleep, N. H. and Biehler, S.: 1970, 'Topography and Tectonics at the Intersections of Fracture Zones and Central Rifts', *J. Geophys. Res.* **75**, 2748–2752.

Stroup, J. B. and Fox, P. J.: 1981, 'Geologic Investigations in the Cayman Trough: Evidence for Thin Crust along the Mid-Cayman Rise', *J. Geol.* **89**, 395–420.

Tamayo Scientific Team: 1984, 'Tectonics at the Intersection of the East Pacific Rise with Tamayo Transform Fault', *Mar. Geophys. Res.* **6**, 159–185 (this issue).

Tchalenko, J. S.: 1970, 'Similarities Between Shear Zones of Different Magnitudes', *Geol. Soc. Amer. Bull.* **81**, 1625–1640.

Tchalenko, J. S. and Ambraseys, N. M.: 1972, 'Structural Analysis of the Dasht-e-Bayaz (Iran) Earthquake Fractures', *Geol. Soc. Amer. Bull.* **81**, 41–60.

Temple, D. G., Scott, R. B. and Rona, P. A.: 1979, 'Geology of a Submarine Hydrothermal Field, Mid-Atlantic Ridge, 25° N Latitude', *J. Geophys. Res.* **84**, 7453–7466.

Whitmarsh, R. B. and Laughton, A. S.: 1976, 'A Long-Range Sonar Study of the Mid-Atlantic Ridge Crest Near 37° N (FAMOUS area) and its Tectonic Implications', *Deep-Sea Res.* **23**, 1005–1023.

Wilcox, R., Harding, T., and Sealy, D. R.: 1973, 'Basic Wrench Tectonics', *Amer. Assoc. Petrol. Geol. Bull.* **57**, 74–96.

Williams, C. A., Louden, K. E., and Tanner, S. J.: 1984, 'The Western Intersection of Oceanographer Fracture Zone with the Mid-Atlantic Ridge', *Mar. Geophys. Res.* **6**, 143–158 (this issue).

Wilson, J. T.: 1965, 'A New Class of Faults and their Bearing on Continental Drift', *Nature* **207**, 343–347.